Made available by Hasselt University Library in https://documentserver.uhasselt.be

Canard cycles of non-linearly regularized piecewise smooth vector fields

Peer-reviewed author version

DE MAESSCHALCK, Peter; HUZAK, Renato & PEREZ, Otavio (2026) Canard cycles of non-linearly regularized piecewise smooth vector fields. In: Journal of Differential Equations, 460 (Art N° 114079).

DOI: 10.1016/j.jde.2025.114079
Handle: http://hdl.handle.net/1942/48157

CANARD CYCLES OF NON-LINEARLY REGULARIZED PIECEWISE SMOOTH VECTOR FIELDS

PETER DE MAESSCHALCK[1], RENATO HUZAK[1] AND OTAVIO HENRIQUE PEREZ[2,1]

Abstract. The main purpose of this paper is to study limit cycles of non-linear regularizations of planar piecewise smooth systems. We deal with a slow-fast Hopf point after non-linear regularization and blow-up. We give a simple criterion for the existence of limit cycles of canard type bluefor a class of (non-linearly) regularized piecewise smooth systems, expressed in terms of zeros of the slow divergence integral. Using the criterion we can construct a quadratic regularization of a piecewise linear center such that for any integer $k > 0$ it has at least $k + 1$ limit cycles, for a suitably chosen monotonic transition function $\varphi_k : \mathbb{R} \to \mathbb{R}$. We prove a similar result for regularized codimension 1 invisible-invisible fold-fold singularities of type II_2. Canard cycles of dodging layer are also considered, and we prove that there can be at most 2 limit cycles (born in a saddle-node bifurcation).

1. Introduction and statement of the problem

In the framework of planar piecewise smooth vector fields (PSVF for short), the fold-fold singularity is known for its rich and interesting bifurcation diagram. Such a singularity can be classified into three cases: visible-visible (VV), visible-invisible (VI) and invisible-invisible (II). Each case has subcases that must be considered depending on the *sliding* and *crossing* regions of the switching locus Σ. For additional information on the bifurcations arising from this type of singularity, see Figure 5 in Section 2.1 and [24, Section 3.2].

It is known that a generic fold-fold singularity has codimension 1. See, for instance, [16, Subsection 4.1.1]. In fact, in the case II, one of the possible subcases is called *non-smooth focus* or *pseudo focus* (which is denoted by II_2 in the above references), since in a small neighborhood of this singularity the switching locus has only crossing points and it presents a focus-like behavior. As discussed in [16, Sections 4 and 7], depending on the coefficients of the Taylor series of the *first return map*, the II_2 fold-fold singularity can have codimension equal or greater than 1. In the codimension 1 case, there is one *crossing limit cycle* bifurcating from it.

In papers [2, 23] the authors provided a systematic analysis of regularizations of PSVFs having a (generic) fold-fold singularity positioned at the origin. Concerning the case II_2, the authors proved the existence of two limit cycles of the regularized system for a suitable *transition function* φ and region of the parameter space (ε, μ), in which ε and μ stand for the singular perturbation and bifurcation parameters, respectively. It is important to remark that the results obtained in [2, 23] concerned the Sotomayor–Teixeira regularization [30] (ST-regularization for short). See also Section 2.

In [29] the authors studied conditions that a PSVF Z must satisfy so that its ST-regularization is structurally stable. Concerning limit cycles, in [29, Proposition 13] the authors proved that hyperbolic crossing limit cycles of Z persist after ST-regularization, for

2020 *Mathematics Subject Classification.* 34D15.

Key words and phrases. Geometric singular perturbation theory, Non-linear regularization, Piecewise smooth vector fields, Slow divergence integral, Slow-fast Hopf point.

.

$\varepsilon > 0$ sufficiently small. One of the limit cycles of the ST-regularized II_2 fold-fold obtained in [2, 23] is related to the crossing one of Z. The second limit cycle is located inside the regularization stripe and its existence depends on the transition function adopted.

Even though the ST-regularization is widely used in both applied and theoretical problems, it is quite natural to ask what happens to the number of limit cycles if one applies other regularization processes. In this paper, our goal is to study planar PSVFs in the presence of fold points and crossing regions via *non-linear regularizations* [21, 25, 28]. See Section 2.2 for a precise definition.

Non-linear regularizations are interesting from both a theoretical and an application point of view. We refer to the book [21], where the author explores how to deal with non-linear regularizations in applications. Moreover, the author addresses the problem of defining the dynamics along the switching manifold. This problem is relevant because there are examples in applied sciences such that the classical Filippov convention does not capture some features of the model under consideration. However, when considering other regularization processes, such features can be taken into account. This fact was also explored in [3], where the authors analyzed a friction oscillator model subject to stiction. Instead of *Filippov solutions*, they introduced the so-called *stiction solutions*, which more accurately reflect the underlying physical behavior. For further discussions on the relation between singular perturbation problems and the dynamics in the switching manifold, see [26]. From those references, it is clear that non-linear regularizations can produce different phenomena which the ST-regularization cannot (see also [27]).

In this paper, we address a question related to the Hilbert's 16th problem: *Is there an upper bound on the number of limit cycles of a regularized piecewise polynomial vector field?* Even though the regularized vector field is not polynomial, such question is still interesting and non trivial as we shall discuss.

In [18], the authors considered a PSVF Z having a fold-fold VI_3 and proved that, for a given integer $k > 0$, there exists a monotonic transition function φ_k such that the ST-regularization of Z has at least $k + 1$ hyperbolic limit cycles. It is important to note that in this reference the PSVF Z is quadratic. Therefore, one could still ask for the maximum number of limit cycles of regularized piecewise linear (PWL for short) systems. In the present paper, we give an answer of this problem in the context of non-linear regularizations of PWL vector fields. Therefore, this paper can also be seen as a continuation of [18].

In Theorem A, we prove that there exist a PWL vector field Z and a continuous combination of degree 2 having the following property: for a given integer $k > 0$, there is a monotonic transition function φ_k such that the non-linear regularization of Z has at least $k + 1$ hyperbolic limit cycles. See Section 2.3 for a precise statement and Section 5.4 for the proof. Moreover, in Theorem A, the PWL vector field is a *non-smooth center*, that is, in a neighborhood of the fold-fold singularity, the PWL vector field presents a center-like behavior. One can see this result as a version of [5, Theorem A] for the non-linearly regularized non-smooth center. More precisely, in [5, Theorem A], for a given positive integer k, the authors explicitly built families of PSVFs with exactly k hyperbolic crossing limit cycles bifurcating from the non-smooth center.

On the other hand, in Theorem B we proved that using non-linear regularizations one can obtain more limit cycles than those 2 obtained in [2, 23] with the ST-regularization of a II_2 singularity of codimension 1. Indeed, there is a PWL vector field Z and a continuous combination of degree 4 having the following property: for a given integer $k > 0$, there exists a monotonic transition function φ_k such that the non-linear regularization of Z has at least $k + 1$ hyperbolic limit cycles. We emphasize that in Theorem B the PWL vector field has

a II_2 singularity of codimension 1. See Section 2.3 for a precise statement and Section 5.5 for the proof. In contrast to the fold-fold singularity of the PWL vector field in Theorem A (which has codimension $k \geq 1$), the fold-fold of the PWL vector field considered in Theorem B has codimension 1. This means that the number of limit cycles of non-linearly regularized PWL vector fields is unbounded even for codimension 1 PWL vector fields.

It is important to remark that this paper focuses on limit cycles of the (non-linearly) regularized PSVF, which is a C^∞-smooth vector field (not polynomial). The limit cycles located within the regularization stripe shrink onto the switching manifold as $\varepsilon \to 0$. Nevertheless, we show that the number of limit cycles in a non-linearly regularized PSVF is unbounded, even when the underlying PSVF Z is piecewise linear. Taking into account that in [18] the authors proved that the number of limit cycles of a ST-regularized quadratic PSVF Z is unbounded, it remains an open question whether the number of limit cycles in ST-regularized PWL vector fields is bounded or not.

Concerning Theorems A and B below, the non-linearly regularized vector field with monotonic transition functions presents a slow-fast Hopf point of the associated slow-fast system (see Section 3.1).

Observe that in [27] the authors proved that, by dropping the monotonicity condition in the ST-regularization, it is possible to generate a (planar) slow-fast jump point (often called SF-generic fold). The same result can be proved for slow-fast Hopf points. In Section 3.1, we prove that slow-fast Hopf points do not appear in ST-regularizations.

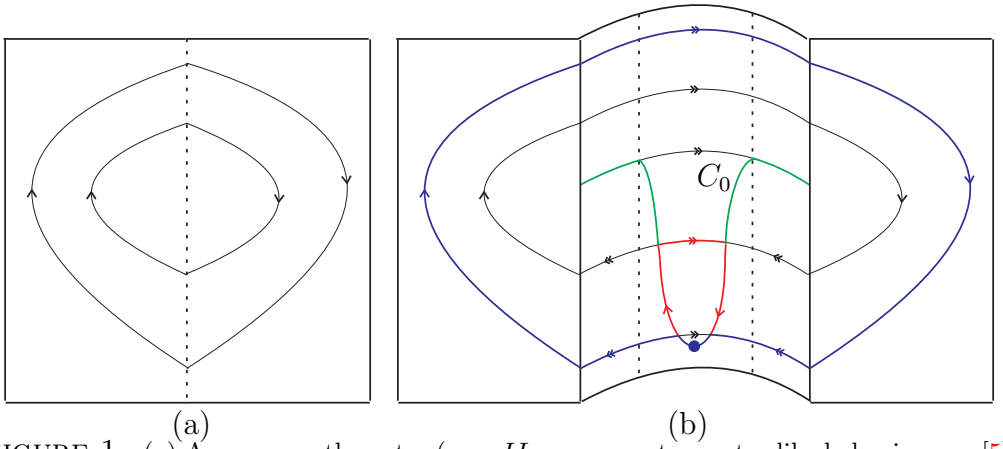

FIGURE 1. (a) A non-smooth center (case II can present a center-like behavior, see [5]). (b) Dynamics on the blow-up cylinder using a non-linear regularization of the non-smooth center. The curve of singularities C_0 contains a normally attracting branch, a normally repelling branch and a slow-fast Hopf point between them. It might produce two different types of canard cycles (red and blue).

The presence of a slow-fast Hopf point (after non-linear regularization and blow-up) plays an important role. The slow-fast Hopf point can generate limit cycles which may grow and become Hausdorff close to canard cycles (see the red graphic in Figure 1(b)). As the size of the canard cycle increases, one can expect limit cycles bifurcating from the blue canard cycle in Figure 1(b). The goal of our paper is to study the number of limit cycles produced by these two types of canard cycles.

Theorem C in Section 5 is a crucial result for proving Theorems A and B. More precisely, we give a simple criterion (expressed in terms of the slow divergence integral) for upper bounds and the existence of limit cycles produced by the blue canard cycle in Figure 1(b). Roughly speaking, if the slow divergence integral has a zero of multiplicity k, then the canard

cycle can produce at most $k+1$ limit cycles (see Theorem C(a)). Simple zeros of the slow divergence integral correspond to hyperbolic limit cycles for unbroken breaking parameter (see Theorem C(b)). An important feature of Theorem C(b) (which is also highlighted in Remark 14) is the following. For a slow-fast Hopf point, if the slow divergence integral has k simple zeros, then one has $k+1$ hyperbolic limit cycles. In the literature [9], this extra limit cycle is the largest; however, in our case, the extra limit cycle will be the smallest due to the geometry of blue canard cycles in Figure 1(b).

Theorem C is stated and proven in a more general setting with two folds, not necessarily of invisible type (see Section 3.3). Indeed, it concerns non-linear regularizations related to the continuous combination given in Equation (8). Such continuous combination can also produce fold-fold of types VV_2 and VI_1 (following the terminology adopted in [24]). We refer to Figure 10(a) in Section 5. A similar criterion has been proven for the red canard cycle in smooth planar slow-fast systems (see e.g. [12]).

Finally, Theorem D in Section 6 deals with canard cycles in case of a dodging layer, given in Figure 10(b). Such canard cycles can produce at most 2 limit cycles and a simple zero of the slow divergence integral corresponds to a codimension 1 bifurcation of limit cycles (saddle-node bifurcation). To the best of our knowledge, this is the first time that canard cycles of dodging layer appears in regularized piecewise smooth vector field. In the smooth setting, canard cycles with a dodging layer have been studied in [9, 31, 32].

We highlight that in previous papers the slow divergence integral was applied near fold-fold singularities having sliding regions. To the best of our knowledge, this is the first time that the slow divergence integral is applied near fold-fold singularities having only crossing regions.

Since the notion of slow divergence integral plays a key role in this paper, we will first explain it for planar smooth slow-fast systems [9, Chapter 5] and regularized planar piecewise smooth systems with sliding [18, 19, 20]. In the planar slow-fast setting and canard theory, the slow divergence integral was developed by De Maesschalck, Dumortier and Roussarie (see [6, 9, 10, 13, 14] and references therein). Consider, for example, the following smooth system with a slow-fast Hopf point at the origin $(x,y)=(0,0)$

$$\begin{cases} \dot{x} = -xy + \varepsilon\left(\alpha - y + y^2 f(y)\right), \\ \dot{y} = x, \end{cases} \tag{1}$$

where $\varepsilon \geq 0$ is the singular perturbation parameter kept small, $\alpha \in \mathbb{R}$ is close to 0 and f is a smooth function. In this paper, by "smooth" we mean C^∞-smooth. If $\varepsilon = 0$ in (1), then we deal with the fast subsystem (often called the fast dynamics). The fast subsystem has the curve of singularities $\{x=0\}$ which is normally attracting when $y>0$ (the nonzero eigenvalue is negative) and normally repelling when $y<0$ (the nonzero eigenvalue is positive). These two branches of the line of singularities are separated by a singularity of nilpotent type at $(0,0)$. The fast fibers are parabolas $x = -\frac{1}{2}y^2 + C$ and the line of singularities has a (quadratic) contact with the fibers at the origin (sometimes we call the origin a contact point). We refer to Figure 2.

An important observation is that, near normally hyperbolic points $y \neq 0$, there exist invariant manifolds of (1) asymptotic to the line $\{x=0\}$ (they correspond to center manifolds if one augments system (1) with $\dot{\varepsilon}=0$). Using standard asymptotic expansions in ε (see e.g. [9]) we obtain

$$x = \varepsilon\left(\frac{\alpha - y + y^2 f(y)}{y} + O(\varepsilon)\right).$$

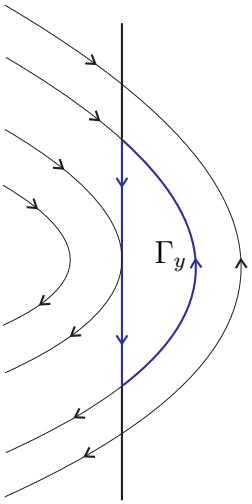

FIGURE 2. Phase portrait of system (1). The canard cycle Γ_y is highlighted in blue.

If we now substitute this for x in the y-component of (1), divide out ε and let ε tend to 0, then we get the slow dynamics [9, Chapter 3]

$$y' = \frac{\alpha - y + y^2 f(y)}{y}, \ y \neq 0,$$

in which the prime $'$ denotes the derivative with respect to the slow time $\tau = \varepsilon t$, where t is the fast time in (1).

Notice that for $\alpha = 0$ the slow dynamics has a removable singularity in $y = 0$ and it is regular there ($y' = -1 + yf(y)$). It is also clear that the slow dynamics points (at least near $y = 0$) from the normally attracting branch $y > 0$ to the normally repelling branch $y < 0$. This produces so-called canard trajectories of (1) which follow the attracting branch, pass through the contact point and then stay close to the repelling branch for some time.

We define now the notion of slow divergence integral [9, Chapter 5]. Suppose that the slow dynamics has no singularities. The slow divergence integral computed along the slow segment $[-y, y] \subset \{x = 0\}$ for $\alpha = 0$ is given by

$$I(y) = \int_y^{-y} \frac{-s ds}{-1 + sf(s)}, \ y > 0.$$

This is an integral of the divergence of (1) for $\varepsilon = 0$ (which is equal to $-y$), with respect to the slow time denoted by τ (which is $d\tau = \frac{dy}{-1+yf(y)}$). It is well-known that zeros of the function I provide candidates for limit cycles of (1), produced by canard cycles. More precisely, for a fixed $y > 0$ and $(\varepsilon, \alpha) = (0, 0)$, the canard cycle Γ_y consists of the segment $[-y, y]$ and the fast orbit connecting $(0, -y)$ and $(0, y)$ (see Figure 2). When I has a zero of multiplicity $k \geq 1$ at $y = y_0$, the canard cycle Γ_{y_0} can generate at most $k + 1$ limit cycles for (ε, α) close to $(0, 0)$ (see [8]).

The notion of slow divergence integral in a regularized piecewise smooth VI_3 model was introduced in [18, 19]. Near the VI_3 fold-fold singularity [18, 24], the Filippov sliding vector field [15] points from the stable sliding region to the unstable sliding region with non-zero speed (see Figure 3(a)).

Notice that the graphic $\widehat{\Gamma}$ in Figure 3(a), consisting of an orbit located in the half-plane $x \geq 0$ with invisible fold point and the portion of $\{x = 0\}$ connecting the end points of

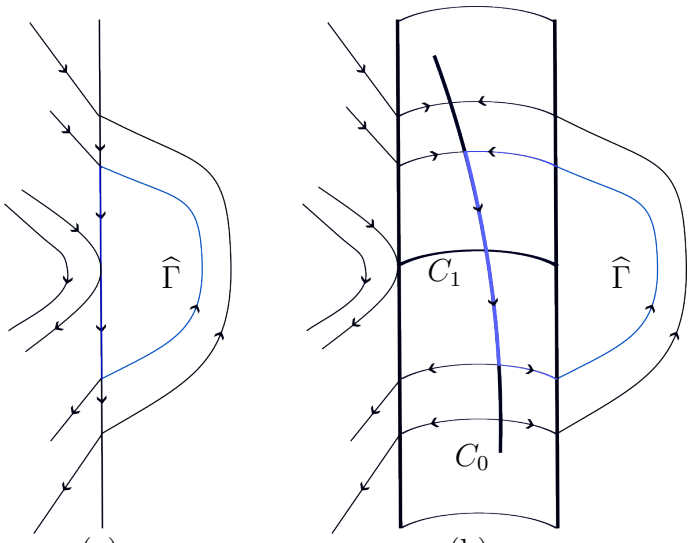

FIGURE 3. (a) The VI_3 fold-fold singularity (the folds have opposite visibility) where $\{x = 0\}$ is the switching line and the Filippov sliding vector field points from the stable sliding region $y > 0$ to the unstable sliding region $y < 0$ with nonzero speed. $\widehat{\Gamma}$ is called a sliding cycle. (b) Dynamics of a regularized VI_3 model on the blow-up cylinder. C_0 and C_1 are curves of singular points.

that orbit, is similar to the canard cycle Γ_y in Figure 2 (the switching line with the Filippov sliding vector field defined on it plays the role of the curve of singularities of (1) with the associated slow dynamics). We call $\widehat{\Gamma}$ a sliding cycle.

Following [18, 19], we can connect $\widehat{\Gamma}$ with the notion of slow divergence integral using a ST-regularization of the VI_3 fold-fold singularity. The ST-regularized system becomes a slow-fast system upon a suitable cylindrical blow-up of the switching line, and then we can compute the slow divergence integral along the slow segment of the blown up sliding cycle $\widehat{\Gamma}$ (see Figure 3(b)). The curve of singularities C_0 of the slow-fast system defined on the blow-up cylinder is normally hyperbolic away from the intersection with C_1 and the flow of the Filippov sliding vector field is the slow dynamics along C_0 (regularly extended through the intersection). In [18, Theorem 3.1], one can find a criterion for the existence of limit cycles of the ST-regularized system produced by sliding cycles. The criterion is expressed in terms of simple zeros of the slow divergence integral. For more details, we refer the reader to [18, 19].

The main purpose of [20], which is a natural continuation of [18], was to introduce the notion of slow divergence integral for the other fold-fold singularities of sliding type VV_1, VI_2, II_1 (see [24] or [20, Figure 2.2]), one-sided tangency points with sliding, etc.

The papers [18, 19, 20] deal with fold-fold singularities of *sliding type*. In this paper, we use the slow divergence integral to study limit cycles in regularized fold-fold singularities of *crossing type*, and we focus our analysis in the II_2 (which is a generic singularity, see [24]) and non-smooth center cases (which is non generic, see [5] and Figure 1(a)). We emphasize that Theorem C can also be used to study the singularities VV_2 and VI_1 (see [24]).

This paper is structured as follows. In Section 2 we present the main tools, such as piecewise smooth vector fields, regularizations and we state Theorems A and B. Section 3 is devoted to defining assumptions of the model that will be studied throughout this paper. We precisely define the types of limit periodic sets that we are interested in in Section 4. Theorems A, B and C are proven in Section 5 and in Section 6 we prove Theorem D. In

this paper, continuous combinations, transition functions, etc., are (C^∞-)smooth. The main reason is that we often refer to [9] where planar slow-fast systems have been studied in the smooth setting.

2. Preliminary definitions and results

Piecewise smooth vector fields are widely adopted to model phenomena of many branches of applied sciences [1, 15]. A closed set with empty interior Σ divides the phase space in finitely many open sets, and on each open set is defined a smooth vector field. In this paper we suppose that the straight line $\Sigma = \{x = 0\}$ divides the phase plane in two open regions, and the smooth vector fields X and Y are defined in the regions $\{x > 0\}$ and $\{x < 0\}$, respectively. In what follows we precisely define this framework using *non-linear regularizations* [25, 28].

2.1. Continuous combinations and piecewise smooth vector fields.

A *continuous combination* is a vector field depending on a parameter λ written as

$$\widetilde{Z}_\mu(\lambda, x, y) = \big(\widetilde{Z}_{1,\mu}(\lambda, x, y), \widetilde{Z}_{2,\mu}(\lambda, x, y)\big),$$

with $\lambda \in \mathbb{R}$, $(x, y) \in U \subset \mathbb{R}^2$, U is an open set and $\mu \in \mathbb{R}^l$ denotes finitely many parameters $\mu = (\mu_1, \ldots, \mu_l)$. Although we assume $\widetilde{Z}$ to be smooth with respect to (λ, x, y, μ), we will keep the terminology *continuous* for two reasons. Firstly, we want to be in accordance with the terminology adopted in [25, 28]. Secondly, being *continuous* extends the notion of being *convex* in a sense that we will soon elucidate.

Define the smooth vector fields

$$\begin{array}{rcccl} X_\mu(x, y) & = & \big(X_{1,\mu}(x, y), X_{2,\mu}(x, y)\big) & := & \widetilde{Z}_\mu(1, x, y), \\ Y_\mu(x, y) & = & \big(Y_{1,\mu}(x, y), Y_{2,\mu}(x, y)\big) & := & \widetilde{Z}_\mu(-1, x, y). \end{array}$$

A piecewise smooth vector field (PSVF for short) is defined as

$$Z_\mu(x, y) = \widetilde{Z}_\mu\Big(\operatorname{sgn}\big(F(x, y)\big), x, y\Big),$$

in which $F : U \subset \mathbb{R}^2 \to \mathbb{R}$ is given by $F(x, y) = x$. It is straightforward to verify that $Z_\mu(x, y) = X_\mu(x, y)$ on $\{F(x, y) > 0\}$ and $Z_\mu(x, y) = Y_\mu(x, y)$ on $\{F(x, y) < 0\}$. One may also denote $Z_\mu = (X_\mu, Y_\mu)$ in order to stress the dependency of Z_μ on the smooth vector fields X_μ and Y_μ. The set $\Sigma = \{F(x, y) = 0\}$ is called *switching set* or *switching manifold*.

Conversely, any given PSVF gives rise to many associated combinations. A well-known example of continuous combination is

$$\widetilde{Z}_\mu(\lambda, x, y) = \frac{1 + \lambda}{2} X_\mu(x, y) + \frac{1 - \lambda}{2} Y_\mu(x, y), \tag{2}$$

which was called *convex combination* in [25, 28]. Replacing λ by $\operatorname{sgn}\big(F(x, y)\big)$ in equation (2), one obtains a PSVF as studied in [16]. In short, the idea of the definition of continuous combination is to allow any curve to connect the points $X_\mu(p)$ and $Y_\mu(p)$, whereas in the convex case a line segment connects such points. See Figure 4.

The *Lie-derivative* of F with respect to the vector field X_μ is given by $X_\mu F = \langle X_\mu, \nabla F\rangle$ and $X_\mu^i F = \langle X_\mu, \nabla X_\mu^{i-1} F\rangle$ for all integers $i \geq 2$. This allows us to define the following regions in Σ:

(1) *Sewing region*: $\Sigma^w = \big\{(x, y) \in \Sigma \ ; \ X_\mu F Y_\mu F > 0\big\}$,
(2) *Sliding region*: $\Sigma^s = \big\{(x, y) \in \Sigma \ ; \ X_\mu F Y_\mu F < 0\big\}$.

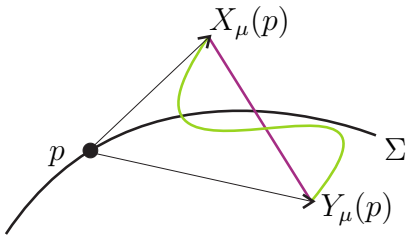

FIGURE 4. Convex and continuous combinations of X_μ and Y_μ.

Following Filippov's convention [15], one can define a vector field in $\Sigma^s \subset \Sigma$. The *Filippov sliding vector field* associated to Z_μ is the vector field $Z_\mu^\Sigma : \Sigma^s \to T\Sigma$ given by

$$Z_\mu^\Sigma(x,y) = \frac{1}{Y_\mu F - X_\mu F}\Big(X_\mu Y_\mu F - Y_\mu X_\mu F\Big).$$

A point $\mathbf{p}_0 \in \Sigma$ is called a *tangency point* if $X_\mu F(\mathbf{p}_0) = 0$ or $Y_\mu F(\mathbf{p}_0) = 0$. A point $\mathbf{p}_0 \in \Sigma$ is a *fold point of* X_μ if $X_\mu F(\mathbf{p}_0) = 0$ and $X_\mu^2 F(\mathbf{p}_0) \neq 0$. If $X_\mu^2 F(\mathbf{p}_0) > 0$, $\mathbf{p}_0$ is a *visible fold of* X_μ and if $X_\mu^2 F(\mathbf{p}_0) < 0$ we say that $\mathbf{p}_0$ is an *invisible fold of* X. Fold points of Y_μ are defined in an analogous way, however $\mathbf{p}_0$ is visible if $Y_\mu^2 F(\mathbf{p}_0) < 0$ and invisible if $Y_\mu^2 F(\mathbf{p}_0) > 0$. If $\mathbf{p}_0$ is a fold of both X_μ and Y_μ simultaneously, then $\mathbf{p}_0$ is called *fold-fold singularity of* Z_μ. This singularity can be classified into three types: visible-visible, visible-invisible and invisible-invisible. See Figure 5.

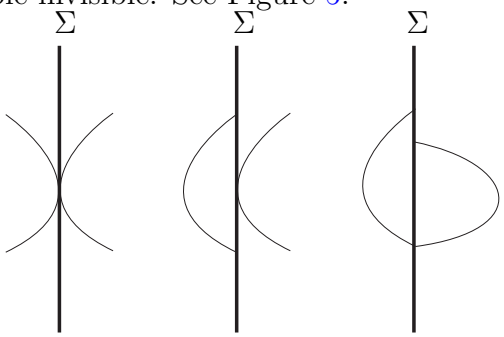

FIGURE 5. Fold-fold singularities. From the left to the right: visible-visible, visible-invisible and invisible-invisible.

2.2. **Regularizations of piecewise smooth vector fields.** We say that $\varphi : \mathbb{R} \to \mathbb{R}$ is a *transition function* if the following conditions are satisfied: **(1)** φ is smooth; **(2)** $\varphi(t) = -1$ if $t \leq -1$ and $\varphi(t) = 1$ if $t \geq 1$. The transition function is *monotonic* if it satisfies **(3)** $\varphi'(t) > 0$ if $s \in (-1, 1)$.

Let $\widetilde{Z}_\mu$ be a continuous combination associated with the PSVF Z_μ. If $\widetilde{Z}_\mu$ is not a convex combination, we say that a φ *non-linear regularization of* Z_μ is the (ε, μ)-family of smooth vector fields given by

$$\widetilde{Z}^\varphi_{\varepsilon,\mu}(x,y) := \widetilde{Z}_\mu\Big(\varphi\Big(\frac{F(x,y)}{\varepsilon}\Big), x, y\Big), \quad 0 < \varepsilon \ll 1. \tag{3}$$

If $\widetilde{Z}_\mu$ is a convex combination, we say that $\widetilde{Z}^\varphi_{\varepsilon,\mu}$ is a φ*-linear regularization of* Z_μ. When $\widetilde{Z}_\mu$ is convex and φ is monotonic, (3) is the well-known *Sotomayor–Teixeira regularization* [30]. We keep the superscript φ in the notation $\widetilde{Z}^\varphi_{\varepsilon,\mu}$ to emphasize the dependency of the regularization on the transition function. Indeed, different transition functions lead to different dynamics of the regularized vector field (see [18, 26, 27]).

In [25, Theorem 1] the authors proved the following result. *Let φ and ψ be monotonic and non-monotonic transition functions, respectively. If $\widetilde{Z}^{\psi}_{\varepsilon,\mu}$ is a ψ-linear regularization, then there exists a unique non-linear regularization $\widetilde{W}^{\varphi}_{\varepsilon,\mu}$ such that $\widetilde{Z}^{\psi}_{\varepsilon,\mu} = \widetilde{W}^{\varphi}_{\varepsilon,\mu}$.* However, in general the converse is not true (see [27, Theorems B and C]).

From now on, we deal with non-linear regularizations in order to obtain richer phenomena, namely *slow-fast Hopf points* (and generic turning points). Indeed, such singularities do not appear in ST regularizations (see Section 3.1).

2.3. **Statement of results.** We are interested in limit cycles of non-linear regularizations as in Figure 1. Such limit cycles can be "large" or "small", as highlighted in blue or red in Figure 1, respectively.

We emphasize that the PSVF's in Theorems A and B are piecewise linear. In addition, in this paper we do not deal with crossing limit cycles, but we are interested in limit cycles of the non-linearly regularized vector field (which is C^{∞}-smooth). If a limit cycle is located inside the regularization stripe, it shrinks to the switching manifold as $\varepsilon \to 0$.

In what follows, the *degree* of a continuous combination is the degree of $\widetilde{Z}_{\mu}$ with respect to the λ variable. In Theorems A and B, the parameter μ is one dimensional. Moreover, we say that an invisible invisible fold-fold singularity is a *codimension* 1 *non-smooth focus* if the first return map ξ of Z_{μ} is given by $\xi(y) = y + ay^2 + O(y^3)$, with $a \neq 0$ (supposing without loss of generality that the fold-fold is positioned in the origin). The invisible invisible fold-fold singularity is a *non-smooth center* if the first return map ξ of Z_{μ} is given by $\xi(y) = y$. The definition of such singularities is also recalled in detail in section 4.

Theorem A. *There exists a continuous combination $\widetilde{Z}_{\mu}$ of degree 2 associated with a linear PSVF Z_{μ} having a non-smooth center such that the following is true: for any integer $k > 0$, there exist a monotonic transition function φ_k and a continuous function $\mu_k : [0, \varepsilon_k] \to \mathbb{R}$, with $\varepsilon_k > 0$, such that the non-linear regularization $\widetilde{Z}^{\varphi_k}_{\varepsilon,\mu_k(\varepsilon)}$ has at least $k+1$ hyperbolic limit cycles, for each $\varepsilon \in (0, \varepsilon_k]$.*

The linear PSVF and continuous combination from Theorem A are given in (26) and (27), respectively. We have a similar result for the singularity II_2.

Theorem B. *There exists a continuous combination $\widetilde{Z}_{\mu}$ of degree at least 4 associated with a linear PSVF Z_{μ} having a codimension 1 non-smooth focus such that the following is true: for any integer $k > 0$, there exist a monotonic transition function φ_k and a continuous function $\mu_k : [0, \varepsilon_k] \to \mathbb{R}$, with $\varepsilon_k > 0$, such that the non-linear regularization $\widetilde{Z}^{\varphi_k}_{\varepsilon,\mu_k(\varepsilon)}$ has at least $k+1$ hyperbolic limit cycles, for each $\varepsilon \in (0, \varepsilon_k]$.*

Concerning Theorems A and B, the following remarks should be made. Firstly, the $k+1$ limit cycles from Theorem A are either produced by red canard cycles in Figure 1 (thus, each of them shrinks to the switching manifold as $\varepsilon \to 0$) or by blue canard cycles in Figure 1. We refer to the proof of Theorem A in Section 5.4. Secondly, the $k+1$ limit cycles from Theorem B shrink to the switching manifold as $\varepsilon \to 0$. For more details see the proof of Theorem B given in Section 5.5.

Our strategy is to define a suitable non-linear regularization such that it presents a generic Hopf turning point. Using tools from geometric singular perturbation theory, in Theorem C in Section 5 we give a simple criterion for detecting such limit cycles, in terms of zeros of the slow divergence integrals. Finally, in Sections 5.4 and 5.5 we show how to construct zeros for the slow divergence integral.

We point out that Theorem C (see also Figure 10(a)) is the main result of this paper which works under very general conditions. It is more convenient to state it later, after we introduce the notion of generic (Hopf) turning point, slow divergence integral, among other tools. We also prove Theorem D in Section 6 for canard cycles of dodging type, see Figure 10(b). Such canard cycles, in contrast to Theorem C, can produce at most 2 limit cycles. Theorem D also contains a simple criterion in terms of the slow divergence integral for existence of saddle node bifurcation of limit cycles.

3. Non-linear regularizations with a generic turning point

In this section, we define a continuous combination whose regularization has a generic turning point positioned at the origin. Such singularity is the subject of subsection 3.1, where we also justify our approach by non-linear regularizations.

3.1. Slow-fast Hopf points.

We say that the 2-dimensional (smooth) slow-fast system

$$\left\{\begin{array}{rcl}\dot{x} &=& f_\mu(x,y,\varepsilon),\\ \dot{y} &=& \varepsilon g_\mu(x,y,\varepsilon),\end{array}\right. \tag{4}$$

has a slow-fast Hopf point positioned at the origin if, for a fixed parameter $\mu=\mu_0$, it satisfies [9, Definition 2.4]

$$\begin{array}{c} f_{\mu_0}(0,0,0)=g_{\mu_0}(0,0,0)=\dfrac{\partial f_{\mu_0}}{\partial x}(0,0,0)=0,\\ \dfrac{\partial^2 f_{\mu_0}}{\partial x^2}(0,0,0)\neq 0, \qquad \left(\dfrac{\partial g_{\mu_0}}{\partial x}(0,0,0)\right)\left(\dfrac{\partial f_{\mu_0}}{\partial y}(0,0,0)\right)<0.\end{array} \tag{5}$$

In Equation (4), the dot $\cdot$ denotes the derivative with respect to the fast time t. Following [9, Section 6.1], a normal form for smooth equivalence for a slow-fast Hopf point is given by

$$\left\{\begin{array}{rcl}\dot{x} &=& y-x^2+x^3h_1(x,\varepsilon,\mu),\\ \dot{y} &=& \varepsilon\Big(a(\mu)-x+x^2h_2(x,\varepsilon,\mu)+yh_3(x,y,\varepsilon,\mu)\Big),\end{array}\right. \tag{6}$$

where functions a,h_1,h_2,h_3 are smooth and $a(\mu_0)=0$. It is straightforward to see that system (6) satisfies conditions (5). The slow-fast Hopf point in (6) is called a generic turning point if $\nabla a(\mu_0)\neq 0$, that is, the function $\mu\mapsto a(\mu)$ is a submersion at $\mu=\mu_0$. In this case we can take $\alpha=a(\mu)$ as a new independent parameter. The parameter α is called a breaking parameter and plays an important role when we want to create limit cycles of (6). We refer to [9, Section 6.3] and later sections for more details. In particular, if $h_2\equiv h_3\equiv 0$ in (6), one obtains a slow-fast classical Liénard equation as studied in [10, 13].

It is well-known that, when considering a regularized vector field as (3), after rescaling of the form $x=\varepsilon\widetilde{x}$ and multiplication by ε one obtains a slow-fast system of the form (4). More specifically, given a PSVF $Z_\mu=(X_\mu,Y_\mu)$ and applying the previous transformation and multiplication in a *linear* regularization, one obtains the system (dropping the tilde to simplify the notation)

$$\left\{\begin{array}{rcl}\dot{x} &=& \dfrac{X_1+Y_1}{2}+\varphi(x)\left(\dfrac{X_1-Y_1}{2}\right),\\ \dot{y} &=& \varepsilon\left(\dfrac{X_2+Y_2}{2}+\varphi(x)\left(\dfrac{X_2-Y_2}{2}\right)\right),\end{array}\right. \tag{7}$$

in which $X=(X_1,X_2)$, $Y=(Y_1,Y_2)$ are applied in $(\varepsilon x,y)$ (we briefly omitted the parameter μ for the sake of simplicity). With this configuration, in which the regularization is linear, the

dynamics on the half cylinder does not present slow-fast Hopf point, with φ being monotonic. This follows directly from the x-component of (7). Indeed, suppose by contradiction that system (7) has a slow-fast Hopf point at the origin. Then one would have

$$\varphi'(0)(X_1 - Y_1)(0,0) = 0, \ \varphi''(0)(X_1 - Y_1)(0,0) \neq 0.$$

Since φ is monotonic (hence, $\varphi'(0) > 0$), this would imply $(X_1 - Y_1)(0,0) = 0$ and $(X_1 - Y_1)(0,0) \neq 0$ simultaneously, which is a contradiction.

As we will see in next subsection, one can generate this kind of point with non-linear regularizations (and monotonic transition functions).

3.2. **Piecewise smooth model.** Motivated by the model (6) given in Section 3.1, we consider the continuous combination

$$\widetilde{Z}_\mu(\lambda, x, y) = \begin{cases} \widetilde{Z}_{1,\mu}(\lambda, x, y) &= y - \lambda^2 + A_\mu(\lambda, x), \\ \widetilde{Z}_{2,\mu}(\lambda, x, y) &= \alpha - \lambda + B_\mu(\lambda, x, y). \end{cases} \tag{8}$$

In Equation (8), we assume $\mu = (\alpha, \widetilde{\mu})$ where the parameter α plays the role of a breaking parameter kept near zero and $\widetilde{\mu} \in \mathbb{R}^{l-1}$ denotes extra parameters. The functions A_μ and B_μ are given by

$$\begin{aligned} A_\mu(\lambda, x) &= \sum_{i=0}^{3} \lambda^{3-i} x^i A_{i,\mu}(\lambda, x), \\ B_\mu(\lambda, x, y) &= \sum_{j=0}^{2} \lambda^{2-j} x^j B_{j,\mu}(\lambda, x) + y B_{3,\mu}(\lambda, x, y), \end{aligned}$$

with $A_{i,\mu}$ and $B_{j,\mu}$ being smooth functions for $i, j = 0, \ldots, 3$. The functions A_μ and B_μ denote higher order terms on the variables λ, x and y, and they can affect the dynamics of the PSVF Z_μ near $\Sigma = \{x = 0\}$. In this case, the PSVF is given by

$$Z_\mu(x, y) = \begin{cases} X_\mu(x, y) = \big(y - 1 + A_\mu(1, x), & \alpha - 1 + B_\mu(1, x, y)\big), \\ Y_\mu(x, y) = \big(y - 1 + A_\mu(-1, x), & \alpha + 1 + B_\mu(-1, x, y)\big). \end{cases} \tag{9}$$

We define a non-linear regularization of $Z_\mu = (X_\mu, Y_\mu)$ as

$$\widetilde{Z}^{\varphi}_{\varepsilon,\mu}(x, y) := \widetilde{Z}_\mu\Big(\varphi\Big(\frac{x}{\varepsilon}\Big), x, y\Big) = \begin{cases} \dot{x} &= y - \varphi^2\left(\frac{x}{\varepsilon}\right) + A_\mu(\varphi\left(\frac{x}{\varepsilon}\right), x), \\ \dot{y} &= \alpha - \varphi\left(\frac{x}{\varepsilon}\right) + B_\mu(\varphi\left(\frac{x}{\varepsilon}\right), x, y), \end{cases} \tag{10}$$

where φ is a transition function (not necessarily monotonic). After rescaling $x = \varepsilon\widetilde{x}$ and multiplication by ε we get (we drop the tilde in order to simplify the notation)

$$\begin{cases} \dot{x} &= y - \varphi^2(x) + A_\mu(\varphi(x), \varepsilon x), \\ \dot{y} &= \varepsilon\left(\alpha - \varphi(x) + B_\mu(\varphi(x), \varepsilon x, y)\right). \end{cases} \tag{11}$$

In what follows, we will define some important assumptions for our proofs. We first state them, and their role will be explained in the sections below.

Given a transition function φ, define the functions

$$F_{\widetilde{\mu}}(x) := \varphi^2(x) - A_{(0,\widetilde{\mu})}(\varphi(x), 0), \quad G_{\widetilde{\mu}}(x) := B_{(0,\widetilde{\mu})}\big(\varphi(x), 0, F_{\widetilde{\mu}}(x)\big) - \varphi(x). \tag{12}$$

For some $0 < M_1, M_2 < 1$, we require the following assumptions for all $x \in [-M_1, M_2]$ and $\mu = \mu_0 = (0, \widetilde{\mu}_0)$ being a parameter defined as in the beginning of Section 3.

(A0) The transition function satisfies $\varphi(0) = 0$ and $\varphi'(0) > 0$.

(A1) $A_{\mu_0}(\pm 1, 0) < 1$.

(A2) The function F defined in (12) satisfies $\frac{F'_{\widetilde{\mu}_0}(x)}{x} > 0$, for all $x \in [-M_1, M_2]$.

(A3) The function G defined in (12) satisfies $\frac{G_{\widetilde{\mu}_0}(x)}{x} < 0$, for all $x \in [-M_1, M_2]$.

Assumption **(A0)** and the definition of A_μ and B_μ imply that the slow-fast system (11) has a generic turning point at the origin for $\mu = \mu_0 = (0, \widetilde{\mu}_0)$. Notice that using a rescaling in (x, y, t) the system (11) can be brought, near the origin, into the normal form (6).

Assumptions **(A0)**, **(A2)**, **(A3)** will be relevant in Section 3.5.1 when we define the notion of slow divergence integral. We use **(A1)** in Section 3.3 when we study tangency points.

3.3. **Tangency points.** Recall that the switching locus is the set $\Sigma = \{x = 0\}$. We are interested in tangency points of the PSVF $Z_\mu = (X_\mu, Y_\mu)$ given by (9). Tangency points of X_μ and Y_μ will be denoted by T_μ^X and T_μ^Y, respectively. It will be clear for the reader that the functions A_μ and B_μ in (9) determine the position and the (in)visibility of fold points, respectively.

Since $X_\mu F = X_{1,\mu}$, the vector field $X_\mu = (X_{1,\mu}, X_{2,\mu})$ is tangent to Σ at points of the form $T_\mu^X = (0, y_\mu^X)$ with

$$y_\mu^X = 1 - A_\mu(1, 0), \tag{13}$$

The second order Lie-derivative at T_μ^X is given by

$$X_\mu^2 F(T_\mu^X) = X_{2,\mu}(T_\mu^X) = \alpha - 1 + B_\mu(1, 0, y_\mu^X),$$

where we used $X_{1,\mu}(T_\mu^X) = 0$ and $\frac{\partial}{\partial y} X_{1,\mu}(x, y) = 1$ (see Equation (9)). This implies that T_μ^X is either a fold point of X_μ or a singularity of X_μ.

Analogously, $Y_\mu F = Y_{1,\mu}$ and tangency points of Y_μ are of the form $T_\mu^Y = (0, y_\mu^Y)$, with

$$y_\mu^Y = 1 - A_\mu(-1, 0), \quad Y_\mu^2 F(T_\mu^Y) = \alpha + 1 + B_\mu(-1, 0, y_\mu^Y), \tag{14}$$

therefore the point T_μ^Y is either a fold point of Y_μ or a singularity of Y_μ.

It can be easily seen that

$$\Sigma^w = \{y < \min\{y_\mu^X, y_\mu^Y\}\} \cup \{y > \max\{y_\mu^X, y_\mu^Y\}\}, \quad \Sigma^s = \{\min\{y_\mu^X, y_\mu^Y\} < y < \max\{y_\mu^X, y_\mu^Y\}\},$$

where Σ^w is the sewing region and Σ^s is the sliding region (see Section 2.1). Notice that $\Sigma^s = \emptyset$ when $y_\mu^X = y_\mu^Y$.

The assumption **(A1)** implies that, for a fixed $\mu = \mu_0 = (0, \tilde{\mu}_0)$, the numbers $y_{\mu_0}^X$ and $y_{\mu_0}^Y$ defined in (13) and (14), respectively, are positive, therefore $T_{\mu_0}^X$ and $T_{\mu_0}^Y$ lie above the generic turning point of (11). This assumption will be important when we define canard cycles as in Figure 10.

3.4. **Scaling the breaking parameter.** Recall the continuous combination $\widetilde{Z}_\mu$ and the PSVF $Z_\mu = (X_\mu, Y_\mu)$ given by (8) and (9), respectively. We introduce the scaling

$$\alpha = \varepsilon \widetilde{\alpha},$$

in which $\widetilde{\alpha} \sim 0$ is called a *regular breaking parameter*. For our purposes we consider a non-linear regularization of $Z_\mu = (X_\mu, Y_\mu)$ as the family $\widetilde{Z}^\varphi_{\varepsilon,\widetilde{\alpha},\widetilde{\mu}}$ given by

$$\widetilde{Z}^\varphi_{\varepsilon,\widetilde{\alpha},\widetilde{\mu}}(x, y) := \widetilde{Z}_{(\varepsilon\widetilde{\alpha},\widetilde{\mu})}\Big(\varphi\Big(\frac{x}{\varepsilon^2}\Big), x, y\Big). \tag{15}$$

Remark 1. In this paper we focus on the regularization $\widetilde{Z}^\varphi_{\varepsilon,\mu}$ defined as in Equation (10), nevertheless, we work with $\widetilde{Z}^\varphi_{\varepsilon,\widetilde{\alpha},\widetilde{\mu}}$ with $\widetilde{\alpha}$ being a regular breaking parameter in Equation (15). The main reason why we work with $\widetilde{Z}^\varphi_{\varepsilon,\widetilde{\alpha},\widetilde{\mu}}$ instead of $\widetilde{Z}^\varphi_{\varepsilon,\mu}$ is that we can then use

results from [6, 12] (after the rescaling $x = \varepsilon^2\widetilde{x}$ and multiplication by ε^2). Due to this fact, we adopt the notation $(\varepsilon\widetilde{\alpha}, \widetilde{\mu})$ instead of μ.

3.5. **Cylindrical blow-up.** In order to study the dynamics of $\widetilde{Z}^{\varphi}_{\varepsilon,\widetilde{\alpha},\widetilde{\mu}}$ near the switching locus $\Sigma = \{x = 0\}$, we perform a *cylindrical blow-up* of the form

$$\begin{array}{rccc} \Phi: & \mathcal{M} & \to & \mathbb{R}^3 \\ & (\tilde{x}, y, \tilde{\varepsilon}, \rho) & \mapsto & (\rho^2\tilde{x}, y, \rho\tilde{\varepsilon}) = (x, y, \varepsilon); \end{array}$$

with $\mathcal{M}$ being a *manifold with corners* (see [22] for details), $(\tilde{x}, \tilde{\varepsilon}) \in \mathbb{S}^1$, $y \in \mathbb{R}$ and $\tilde{\varepsilon}, \rho \geq 0$. This blow-up has a slightly different expression from the usual approach [4] (it is quasi-homogeneous instead of homogeneous). The *blown-up vector field* is defined as the pullback of $\widetilde{Z}^{\varphi}_{\varepsilon,\widetilde{\alpha},\widetilde{\mu}} + 0\frac{\partial}{\partial\varepsilon}$ multiplied by ρ^2:

$$Z^{\varphi}_{\widetilde{\alpha},\widetilde{\mu}} := \rho^2\Phi^*\left(\widetilde{Z}^{\varphi}_{\varepsilon,\widetilde{\alpha},\widetilde{\mu}} + 0\frac{\partial}{\partial\varepsilon}\right).$$

In Sections 3.5.1–3.5.3, we study the dynamics of $Z^{\varphi}_{\widetilde{\alpha},\widetilde{\mu}}$ near the exceptional divisor $\mathcal{C} = \{\Phi^{-1}(\Sigma \times \{0\})\}$, which is a half-cylinder (see Figure 6). This study is carried out using directional charts.

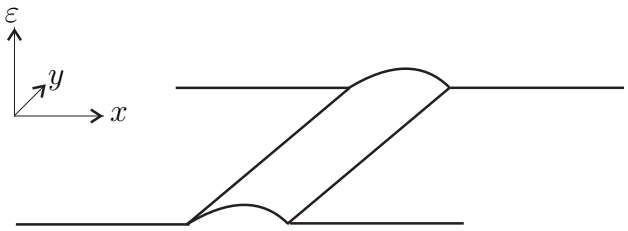

FIGURE 6. Blowing up the switching line Σ.

3.5.1. *Dynamics in the chart* $\tilde{\varepsilon} = 1$. In this scaling chart we have $x = \varepsilon^2 x_2$ where (x_2, y) is kept in a large compact set in $\mathbb{R}^2$ and $\varepsilon > 0$ is small. The vector field $\widetilde{Z}^{\varphi}_{\varepsilon,\widetilde{\alpha},\widetilde{\mu}} + 0\frac{\partial}{\partial\varepsilon}$ yields (after multiplication by the positive factor ε^2) to

$$\left\{\begin{array}{rcl} \dot{x}_2 &=& y - \varphi^2(x_2) \quad + \quad A_{(\varepsilon\widetilde{\alpha},\widetilde{\mu})}\left(\varphi(x_2), \varepsilon^2 x_2\right), \\ \dot{y} &=& \varepsilon^2\Big(\varepsilon\widetilde{\alpha} - \varphi(x_2) \quad + \quad B_{(\varepsilon\widetilde{\alpha},\widetilde{\mu})}\left(\varphi(x_2), \varepsilon^2 x_2, y\right)\Big), \end{array}\right. \tag{16}$$

with $\dot{\varepsilon} = 0$ (ε is the singular perturbation parameter). In equation (16), the dot $\cdot$ denotes the derivative with respect to the fast time t. For $\varepsilon = 0$, equation (16) turns to

$$\left\{\begin{array}{rcl} \dot{x}_2 &=& y - \varphi^2(x_2) \quad + \quad A_{(0,\widetilde{\mu})}(\varphi(x_2), 0), \\ \dot{y} &=& 0. \end{array}\right. \tag{17}$$

The curve of singularities of (17) is given by $C_0 = \left\{y = F_{\widetilde{\mu}}(x_2)\right\}$, where $F_{\widetilde{\mu}}$ is defined in (12). The curve C_0 contains two horizontal portions $\{y = y^X_{(0,\widetilde{\mu})}, x_2 \geq 1\}$ and $\{y = y^Y_{(0,\widetilde{\mu})}, x_2 \leq -1\}$, where $y^X_{(0,\widetilde{\mu})}$ is defined in (13) and $y^Y_{(0,\widetilde{\mu})}$ in (14). See Figure 7 and Remark 2.

Recall that in the interval $(-1, 1)$ we adopt Assumption **(A2)**. Assumption **(A2)** is true locally near $x_2 = 0$, due to Assumption **(A0)**. The Assumption **(A2)** implies that for each $\widetilde{\mu} \sim \widetilde{\mu}_0$ the curve C_0 has a parabola-like shape inside the segment $[-M_1, M_2]$ with a normally attracting branch ($x_2 \in (0, M_2]$) and a normally repelling branch ($x_2 \in [-M_1, 0)$).

It is clear that the transition function φ has to be monotonic on $[-M_1, M_2]$ (not necessarily monotonic outside this segment).

The slow dynamics [9, Chapter 3] along the segment $[-M_1, M_2]$ is given by

$$x_2' = \frac{dx_2}{d\tau} = \frac{G_{\widetilde{\mu}}(x_2)}{F'_{\widetilde{\mu}}(x_2)}, \tag{18}$$

in which $\tau = \varepsilon^2 t$ stands for the slow time. The Assumption **(A3)** defined in Section 3.2 assures that the slow dynamics (18) is regular for all $x_2 \in [-M_1, M_2]$ and points from the attracting branch to the repelling branch. With this setting, the origin of (16) is a generic Hopf turning point and the slow dynamics is regular in $[-M_1, M_2]$.

The following slow divergence integrals [9, Chapter 5] (see also [10]) play an important role in this paper:

(19)
$$I^+_{\widetilde{\mu}}(x_2) := -\int_{x_2}^{0} \frac{F'_{\widetilde{\mu}}(s)^2}{G_{\widetilde{\mu}}(s)} ds < 0,\ x_2 \in (0, M_2], \quad I^-_{\widetilde{\mu}}(x_2) := -\int_{x_2}^{0} \frac{F'_{\widetilde{\mu}}(s)^2}{G_{\widetilde{\mu}}(s)} ds < 0,\ x_2 \in [-M_1, 0).$$

These are integrals of the divergence of the vector field (17), computed along C_0 with respect to the slow time τ. More precisely, the integral $I^+_{\widetilde{\mu}}(x_2)$ is computed along the attracting segment $[0, x_2] \subset [0, M_2]$ and $I^-_{\widetilde{\mu}}(x_2)$ along the repelling segment $[x_2, 0] \subset [-M_1, 0]$. See also Sections 5 and 6.

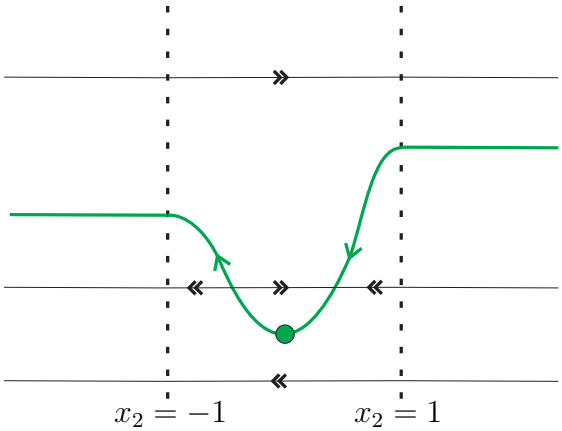

FIGURE 7. Phase portrait of (17) (the family chart $\tilde{\varepsilon} = 1$).

Remark 2. The existence of the degenerate (nonhyperbolic) horizontal lines in Figure 7 is due to the way that we defined the transition function φ. Observe that $\varphi(t) \equiv -1$ when $t \leq -1$ and $\varphi(t) \equiv 1$ when $t \geq 1$ (see Section 2.2). Now, since $\varphi \equiv$ constant for $|x_2| \geq 1$, then the critical curve C_0 is given by horizontal curves in the region $|x_2| \geq 1$. These horizontal lines will be visible in the phase directional charts $\tilde{x} = \pm 1$ studied below.

3.5.2. *Dynamics in the chart* $\tilde{x} = 1$. In this chart we have $(x, \varepsilon) = (\rho_3^2, \rho_3\varepsilon_3)$. The vector field $\widetilde{Z}^{\varphi}_{\varepsilon,\widetilde{\alpha},\widetilde{\mu}} + 0\frac{\partial}{\partial\varepsilon}$ changes, after multiplication by ρ_3^2, into

$$\left\{\begin{array}{rcl} \dot{\rho}_3 &=& \rho_3 H_{\widetilde{\alpha},\widetilde{\mu}}(\rho_3, y, \varepsilon_3), \\ \dot{y} &=& \rho_3^2\Big(\rho_3\varepsilon_3\widetilde{\alpha} - \varphi\big(\frac{1}{\varepsilon_3^2}\big) + B_{(\rho_3\varepsilon_3\widetilde{\alpha},\widetilde{\mu})}\Big(\varphi\big(\frac{1}{\varepsilon_3^2}\big), \rho_3^2, y\Big)\Big), \\ \dot{\varepsilon}_3 &=& -\varepsilon_3 H_{\widetilde{\alpha},\widetilde{\mu}}(\rho_3, y, \varepsilon_3), \end{array}\right. \tag{20}$$

in which

$$H_{\widetilde{\alpha},\widetilde{\mu}}(\rho_3, y, \varepsilon_3) = \frac{1}{2}\Big(y - \varphi^2\big(\frac{1}{\varepsilon_3^2}\big) + A_{(\rho_3\varepsilon_3\widetilde{\alpha},\widetilde{\mu})}\Big(\varphi\big(\frac{1}{\varepsilon_3^2}\big), \rho_3^2\Big)\Big).$$

Observe that in (20) we can set $\varphi\big(\frac{1}{\varepsilon_3^2}\big) = 1$ for $0 \leq \varepsilon_3 \leq 1$. The line $\{\rho_3 = \varepsilon_3 = 0\}$ consists of singularities of (20). The Jacobian matrix of (20) evaluated in $(0, y, 0)$ is given by

$$J_3 = \begin{pmatrix} \frac{y - y^X_{(0,\widetilde{\mu})}}{2} & 0 & 0 \\ 0 & 0 & 0 \\ 0 & 0 & -\frac{y - y^X_{(0,\widetilde{\mu})}}{2} \end{pmatrix},$$

which means that all the singularities are semi-hyperbolic, except for $T^X_{(0,\widetilde{\mu})} = (0, y^X_{(0,\widetilde{\mu})}, 0)$ where we deal with a degenerate singularity.

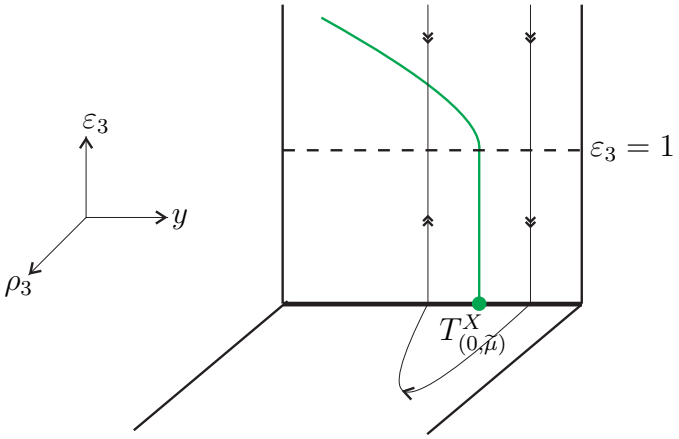

FIGURE 8. Phase portrait of (20) (the chart $\tilde{x} = 1$). On the invariant plane $\{\rho_3 = 0\}$ one obtains a smooth curve of singularities given by $\{H_{\widetilde{\alpha},\widetilde{\mu}}(0, y, \varepsilon_3) = 0\}$. Such curve is a straight segment for $0 \leq \varepsilon_3 \leq 1$ and it contains the point $T^X_{(0,\widetilde{\mu})}$.

3.5.3. *Dynamics in the chart* $\tilde{x} = -1$. Using $(x, \varepsilon) = (-\rho_1^2, \rho_1\varepsilon_1)$ one obtains, after multiplication by ρ_1^2, the system

$$\left\{ \begin{array}{rcl} \dot{\rho}_1 &=& -\rho_1 G_{\widetilde{\alpha},\widetilde{\mu}}(\rho_1, y, \varepsilon_1), \\ \dot{y} &=& \rho_1^2\Big(\rho_1\varepsilon_1\widetilde{\alpha} - \varphi\big(-\frac{1}{\varepsilon_1^2}\big) + B_{(\rho_1\varepsilon_1\widetilde{\alpha},\widetilde{\mu})}\Big(\varphi\big(-\frac{1}{\varepsilon_1^2}\big), -\rho_1^2, y\Big)\Big), \\ \dot{\varepsilon}_1 &=& \varepsilon_1 G_{\widetilde{\alpha},\widetilde{\mu}}(\rho_1, y, \varepsilon_1), \end{array} \right. \tag{21}$$

in which

$$G_{\widetilde{\alpha},\widetilde{\mu}}(\rho_1, y, \varepsilon_1) = \frac{1}{2}\Big(y - \varphi^2\big(-\frac{1}{\varepsilon_1^2}\big) + A_{(\rho_1\varepsilon_1\widetilde{\alpha},\widetilde{\mu})}\Big(\varphi\big(-\frac{1}{\varepsilon_1^2}\big), -\rho_1^2\Big)\Big).$$

One can set $\varphi\big(-\frac{1}{\varepsilon_1^2}\big) = -1$ for $0 \leq \varepsilon_1 \leq 1$ and the phase-portrait of Equation (21) can be sketched analogously as it was described in Subsection 3.5.2.

4. Candidates for canard cycles

Recall that $\alpha = \varepsilon\widetilde{\alpha}$, and we are considering the parameter μ as $\mu = (\alpha, \widetilde{\mu}) = (\varepsilon\widetilde{\alpha}, \widetilde{\mu})$. See also the beginning of Subsection 3.4.

Consider the dynamics on the top of the half cylinder as described in Subsection 3.5.1. Since the origin is a generic Hopf turning point, it is clear that one can expect creation of limit cycles inside the region $|x_2| < 1$ (recall Figure 7). However, we also want to study

"big" limit cycles in the sense that they are not strictly contained inside the regularization stripe. In what follows, we precisely define the shape of the limit periodic sets (called canard cycles), at level $\varepsilon = 0$ and $\widetilde{\mu} = \widetilde{\mu}_0$, that we are interested in. Two cases will be considered: *terminal* and *dodging cases*. This terminology is inspired by [9, Lemma 5.3].

Define the *half return map of* $X_{(0,\widetilde{\mu})}$ (when it exists) as

$$\begin{array}{rccl} \xi_X: & S_0 \subset \Sigma & \to & \{y < y^X_{(0,\widetilde{\mu})}\} \subset \Sigma \\ & p = (0,y) & \mapsto & \xi_X(y) = \pi_2\Big(\phi_X\big(t(p),p\big)\Big), \end{array}$$

in which S_0 is a bounded segment contained in $\{y > y^X_{(0,\widetilde{\mu})}\}$ for each $\widetilde{\mu}$ close to $\widetilde{\mu}_0$, π_2 is the projection in the second coordinate, ϕ_X is the flow of $X_{(0,\widetilde{\mu})}$, and $t(p) > 0$ denotes the smallest (and finite) time in which the flow by p intersects Σ. The half return map ξ_X defined as above is smooth. The *half return map of* $Y_{(0,\widetilde{\mu})}$ is denoted by ξ_Y and it is defined in the same fashion, but we consider the flow of $Y_{(0,\widetilde{\mu})}$ in backward time instead. See Figure 9. The half return maps will depend on the parameter $\widetilde{\mu}$. However, for the sake of simplicity, we will denote them by $\xi_{X,Y}$.

(A4) Let $\widetilde{\mu} = \widetilde{\mu}_0$ and let $[-M_1, M_2]$ be the segment fixed in **(A2)** and **(A3)**.

(1) **(Terminal case)** We assume that $\xi_X(y) \in (0, y^X_{(0,\widetilde{\mu}_0)})$ (resp. $\xi_Y(y) \in (0, y^Y_{(0,\widetilde{\mu}_0)})$) for each $y \in S_0$ where $\xi_X(y)$ (resp. $\xi_Y(y)$) is the y-value of the first intersection with the y-axis of the forward (resp. backward) flow of $(0,y)$ following $X_{(0,\widetilde{\mu}_0)}$ (resp. $Y_{(0,\widetilde{\mu}_0)}$). Moreover, we assume that the unstable (resp. stable) manifold of the saddle singularity $(\rho_3, y, \varepsilon_3) = (0, \xi_X(y), 0)$ (resp. $(\rho_1, y, \varepsilon_1) = (0, \xi_Y(y), 0)$) of (20) (resp. (21)) hits the attracting (resp. repelling) branch of the curve of singularities C_0 of (17) on the blow-up locus at a point $p_+ \in C_0$ (resp. $p_- \in C_0$) with the x_2 coordinate contained in the interval $(0, M_2]$ (resp. $[-M_1, 0)$).

(2) **(Dodging case)** Let $y^Y_{(0,\widetilde{\mu}_0)} < y^X_{(0,\widetilde{\mu}_0)}$. We assume that $\xi_Y(y) \in (0, y^Y_{(0,\widetilde{\mu}_0)})$ for each $y \in S_0$ and the stable manifold of the saddle singularity $(\rho_1, y, \varepsilon_1) = (0, \xi_Y(y), 0)$ of (21) hits the repelling branch of C_0 on the blow-up locus at a point $p_- \in C_0$ with the x_2 coordinate contained in the $[-M_1, 0)$. Furthermore, we assume that for each $y \in S_0$ the horizontal orbit of (17) through $(0,y)$ hits the attracting branch of C_0 at a point $p_+ \in C_0$ with the x_2 coordinate contained in $(0, M_2]$.

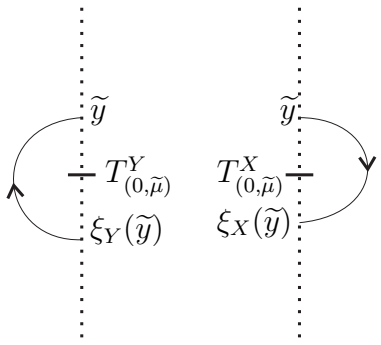

FIGURE 9. Half-return maps ξ_X and ξ_Y. Such maps are defined by considering the flow of $X_{(0,\widetilde{\mu})}$ and $Y_{(0,\widetilde{\mu})}$ in forward and backward time, respectively.

In the terminal case, we assume that both ξ_X and ξ_Y are well defined on S_0. Using the assumptions **(A0-4)** we can define a canard cycle as follows (see Figure 10(a)). Let

$\widetilde{y} \in S_0$. The canard cycle at level $\widetilde{y}$ consists of a fast orbit $y = \widetilde{y}$ located on the cylinder, the orbit connecting the corner points of the cylinder $(\rho_3, y, \varepsilon_3) = (0, \widetilde{y}, 0)$ and $(\rho_3, y, \varepsilon_3) = (0, \xi_X(\widetilde{y}), 0)$, the orbit connecting $(\rho_3, y, \varepsilon_3) = (0, \xi_X(\widetilde{y}), 0)$ and p_+, the portion of the curve of singularities C_0 between p_+ and p_-, the orbit connecting p_- and the corner point of the cylinder $(\rho_1, y, \varepsilon_1) = (0, \xi_Y(\widetilde{y}), 0)$ and the orbit connecting $(\rho_1, y, \varepsilon_1) = (0, \xi_Y(\widetilde{y}), 0)$ and $(\rho_1, y, \varepsilon_1) = (0, \widetilde{y}, 0)$. We denote this canard cycle by $\Upsilon^{\widetilde{y}}$. Notice that the slow dynamics defined along the portion of C_0 between p_+ and p_- points from the right to the left. Thus, the canard cycle $\Upsilon^{\widetilde{y}}$ can produce limit cycles of $\widetilde{Z}^{\varphi}_{\varepsilon,\widetilde{\alpha},\widetilde{\mu}}$, for $\varepsilon > 0$, $\widetilde{\alpha} \sim 0$ and $\widetilde{\mu}$ close to $\widetilde{\mu}_0$ (see Theorem C).

Now, we describe the dodging case (see Figure 10(b)). The canard cycle at level $\widetilde{y} \in S_0$ consists of a fast horizontal orbit of (17) through $(0, \widetilde{y})$, the portion of the curve of singularities C_0 between p_+ and p_-, the orbit connecting p_- and the corner point of the cylinder $(\rho_1, y, \varepsilon_1) = (0, \xi_Y(\widetilde{y}), 0)$ and the orbit connecting $(\rho_1, y, \varepsilon_1) = (0, \xi_Y(\widetilde{y}), 0)$ and $(\rho_1, y, \varepsilon_1) = (0, \widetilde{y}, 0)$. We denote this canard cycle by $\Gamma^{\widetilde{y}}$ and it can produce limit cycles of $\widetilde{Z}^{\varphi}_{\varepsilon,\widetilde{\alpha},\widetilde{\mu}}$ (see Theorem D). Note that the half return map ξ_Y has to be well defined on S_0 (see assumption **(A4)**).

It is clear that we can use a similar definition of $\Gamma^{\widetilde{y}}$ when $y^X_{(0,\widetilde{\mu}_0)} < y^Y_{(0,\widetilde{\mu}_0)}$ and the same results can be proved (in assumption **(A4)**, we use the half return map ξ_X instead of ξ_Y).

There are some degenerate canard cycles in the singular limit $\varepsilon = 0$ that can also produce limit cycles for $\varepsilon > 0$, but they are beyond the scope of this paper. They are degenerate in the sense that they require further blow-up analysis in order to define transition maps. Such degenerate cases are characterized by having fast orbit segments in the level $y = y^X_{(0,\widetilde{\mu}_0)}$ or $y = y^Y_{(0,\widetilde{\mu}_0)}$ on the top of the cylinder. See Figure 11.

Remark 3. When the PSVF Z_μ has a non-smooth center or focus (see Theorems A and B), the half return maps $\xi_{X,Y}$ are well defined. The continuous combination (8) is more general than it appears and it is possible that ξ_X or ξ_Y (or both $\xi_{X,Y}$) are not well defined even when assumptions **(A0-3)** are satisfied. Indeed, it is not difficult to find suitable functions $A_\mu(\lambda, x)$ and $B_\mu(\lambda, x, y)$ such that the associated PSVF Z_μ has a fold-fold of types VV_2 or VI_1 (following the terminology adopted in [24]) where the half return maps are not necessarily well defined. We therefore assume that **(A4)** is also satisfied such that canard cycles in terminal or dodging case exist.

The *first return map of* $Z_{(0,\widetilde{\mu})}$ is given by $\xi = \xi_Y^{-1} \circ \xi_X$ (when it is well defined). When $T^X_{(0,\widetilde{\mu})} = T^Y_{(0,\widetilde{\mu})}$ are both invisible fold points and $\xi(y) = y + ay^2 + O(y^3)$ with $a \neq 0$ (after a translation of $T^{X,Y}_{(0,\widetilde{\mu})}$ to the origin), then the invisible-invisible fold-fold has codimension 1, and it was denoted by II_2 in [24] (see also [16]). Such singularity present a focus-like behavior. Moreover, if $a < 0$ then the singularity is an attracting non-smooth focus and it is a repelling one otherwise. If $\xi(y) = Id$, then the invisble-invisible fold-fold is a non-smooth center [5].

5. Analysis of the terminal case

In this section, we prove that the slow divergence integral can indeed be used to detect limit cycles of the regularized vector field $\widetilde{Z}^{\varphi}_{\varepsilon,\widetilde{\alpha},\widetilde{\mu}}$ (as in (15)), for ε small and positive. Firstly, we consider the terminal case defined in Section 4 and assume that assumptions **(A0-4)** are satisfied. We fix the closed interval S_0 from **(A4)**.

The transversal sections will be denoted by $\sigma_i^{\pm}$ for $i = 0, \ldots, 5$, and we simply denote $\sigma_0^{\pm} = \sigma_0$ and $\sigma_5^{\pm} = \sigma_5$. The transition maps will be denoted by $\Pi_i^{\pm} : \sigma_{i-1}^{\pm} \to \sigma_i^{\pm}$ for

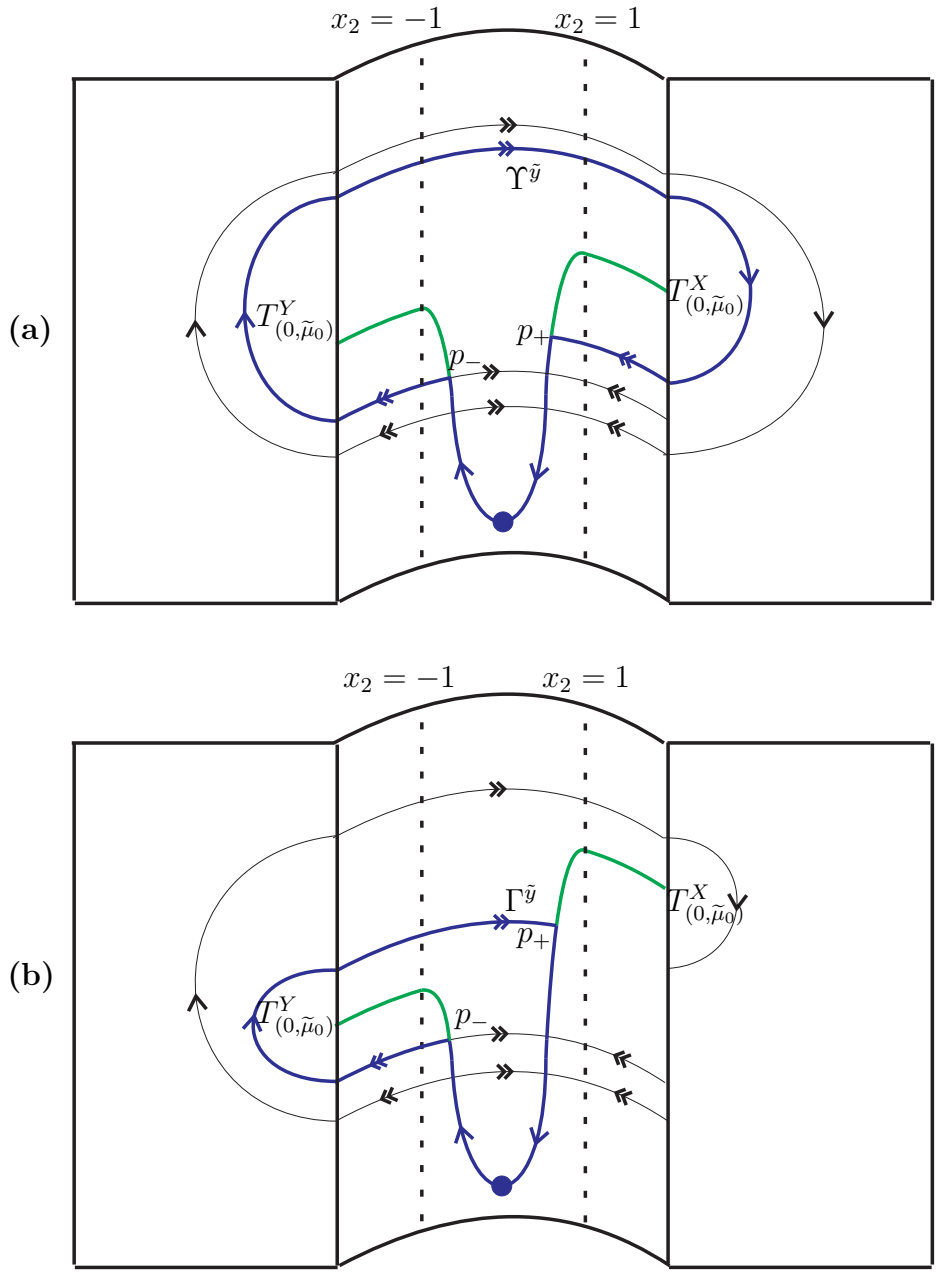

FIGURE 10. Canard cycles $\Upsilon^{\tilde{y}}$ and $\Gamma^{\tilde{y}}$ (highlighted in blue) that can produce limit cycles of $\widetilde{Z}^{\varphi}_{\varepsilon,\tilde{\alpha},\tilde{\mu}}$. Figures (a) and (b) (on the top and on the bottom, respectively) show the terminal and dodging cases, respectively.

$i = 1, \ldots, 5$. We will compute the transversal sections and transition maps in the right-hand side of Figure 12(a). The study of the left hand side is completely analogous.

5.1. **Sections and transitions on the family chart $\tilde{\varepsilon} = 1$.** In this family chart, we define the sections (as sketched in Figure 12(a))

$$\begin{aligned} \sigma_0 &= \{x_2 = 0, \quad 0 \le \varepsilon < \varepsilon_0, \quad y \in S_0\}, \\ \sigma_1^+ &= \{x_2 = \bar{x}_2, \quad 0 \le \varepsilon < \varepsilon_0, \quad y \in S_1\}, \\ \sigma_4^+ &= \{x_2 = \bar{x}_2, \quad 0 \le \varepsilon < \varepsilon_0, \quad y \in S_4\}, \end{aligned}$$

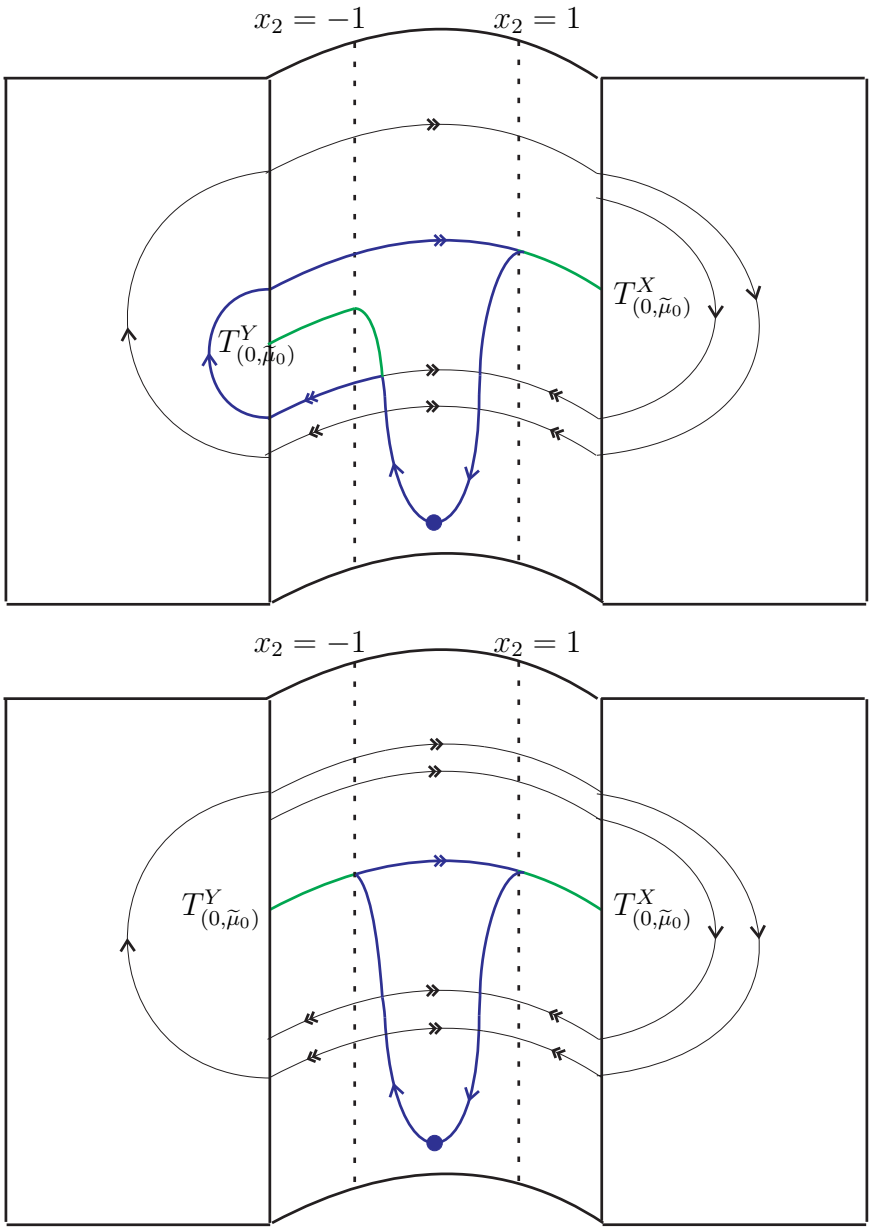

FIGURE 11. Degenerate canard cycles (highlighted in blue) that can produce limit cycles of $\widetilde{Z}^{\varphi}_{\varepsilon,\widetilde{\alpha},\widetilde{\mu}}$.

in which $\bar{x}_2 > 1$ is large and fixed and ε_0 is small. Moreover, S_1 and S_4 are appropriate open intervals such that $S_0 \subset S_1$ and the horizontal orbit of (17) through $(x_2, y) = (\bar{x}_2, y)$, $y \in S_4$, hits the attracting branch of the curve of singularities C_0 at a point with the x_2-value contained in the interval $(0, M_2]$. The sections σ_0, σ_1^+ and σ_4^+ are parametrized by the variable y. Following [6], the section σ_5 is defined near the generic turning point $(x_2, y) = (0, 0)$, but in a new phase space $(\hat{x}_2, \hat{y})$ after applying the rescaling $(x_2, y) = (\varepsilon^2\hat{x}_2, \varepsilon\hat{y})$ to (16) and dividing the new system by $\varepsilon > 0$. Then we take $\sigma_5 = \{\hat{x}_2 = 0,\ 0 \leq \varepsilon < \varepsilon_0,\ \hat{y} \in \mathbb{R}\}$.

We have the following Lemma.

Lemma 4. *The transition map* $\Pi_1^+ : \sigma_0 \to \sigma_1^+$, $(y, \varepsilon) \mapsto (\pi_1^+(y, \varepsilon, \widetilde{\alpha}, \widetilde{\mu}), \varepsilon)$, *is well defined and is* C^∞.

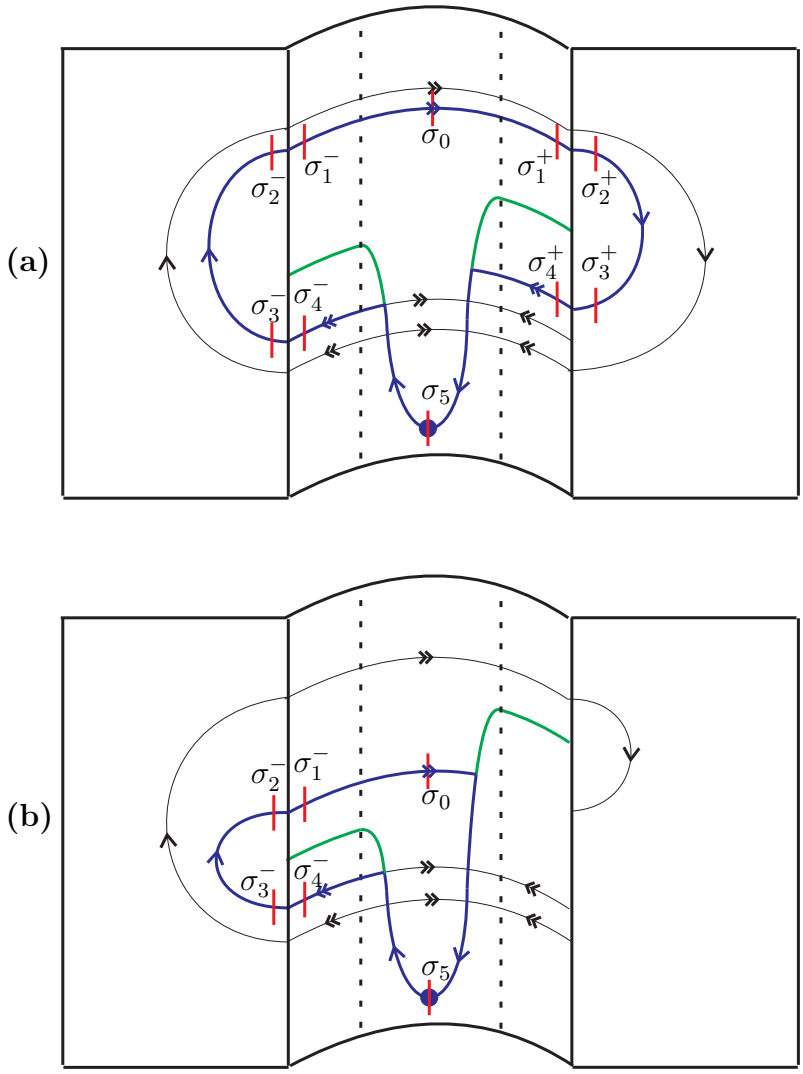

FIGURE 12. Transversal sections highlighted in red. Figures (a) and (b) represent terminal and dodging cases, respectively. We sketched σ_5 as a small segment in order to simplify it to the reader.

Proof. The transition map Π_1^+ is defined by following trajectories of the slow-fast system (16) between σ_0 and σ_1^+. Since (16) is regular in this region, the statement is true. □

Since the origin of (16) is a generic Hopf turning point and the slow dynamics is regular in $[-M_1, M_2]$, then we are in the framework of [6]. Therefore, by [6, Theorem 4] one obtains the transition map $\Pi_5^+ : \sigma_4^+ \to \sigma_5$ and its properties. This transition map is defined by following the orbits of (16) between sections σ_4^+ and σ_5. See Lemma 5 below.

In what follows, we define

$$I_5^{\pm}(y, \widetilde{\mu}) := I_{\widetilde{\mu}}^{\pm}(x_2^{\pm}(y)), \tag{22}$$

where $I_{\widetilde{\mu}}^+$ (resp. $I_{\widetilde{\mu}}^-$) is the slow divergence integral (19) and $x_2^+(y) > 0$ (resp. $x_2^-(y) < 0$) is the x_2-coordinate of the ω-limit point (resp. α-limit point) of the fast orbit of (17) through $y \in \sigma_4^+$ (resp. $y \in \sigma_4^-$). Clearly, we have $F_{\widetilde{\mu}}(x_2^{\pm}(y)) = y$ with $F_{\widetilde{\mu}}$ defined in (12).

Lemma 5. *The $\hat{y}$-component of the transition map $\Pi_5^+ : \sigma_4^+ \to \sigma_5$, $(y,\varepsilon) \mapsto (\pi_5^+(y,\varepsilon,\widetilde{\alpha},\widetilde{\mu}),\varepsilon)$, is given by*

$$\pi_5^+(y,\varepsilon,\widetilde{\alpha},\widetilde{\mu}) = f_5^+(\varepsilon,\widetilde{\alpha},\widetilde{\mu}) - \exp\left(\frac{I_5^+(y,\widetilde{\mu}) + \Psi_1^+(y,\varepsilon,\widetilde{\alpha},\widetilde{\mu}) + \Psi_2^+(\varepsilon,\widetilde{\alpha},\widetilde{\mu})\varepsilon^2 \ln\varepsilon}{\varepsilon^2}\right),$$

in which $I_5^+(y,\widetilde{\mu}) < 0$ is the slow divergence integral (22). The functions $\Psi_{1,2}^+$ and f_5^+ are smooth, and Ψ_1^+ is $O(\varepsilon)$.

Remark 6. The minus sign in the front of the exponential in Lemma 5 is due to the chosen orientation of parametrization of σ_5.

To study the transitions $\Pi_{2,3,4}^+$ we will work on chart $\tilde{x} = 1$.

5.2. **Sections and transitions on the family chart $\tilde{x} = 1$.** Firstly, we rewrite the transversal sections $\sigma_{1,4}^+$ in this system of coordinates (recall the directional charts described in subsection 3.4):

$$\begin{aligned}\sigma_1^+ &= \{0 \le \rho_3 < \varepsilon_0\sqrt{\bar{x}_2},\quad \varepsilon_3 = \tfrac{1}{\sqrt{\bar{x}_2}},\quad y \in S_1\},\\ \sigma_4^+ &= \{0 \le \rho_3 < \varepsilon_0\sqrt{\bar{x}_2},\quad \varepsilon_3 = \tfrac{1}{\sqrt{\bar{x}_2}},\quad y \in S_4\},\end{aligned}$$

in which $\bar{x}_2 > 1$. We further define the following transversal sections, with $\tilde{\rho}_3$ being a small and positive constant:

$$\begin{aligned}\sigma_2^+ &= \{\rho_3 = \tilde{\rho}_3,\quad 0 \le \varepsilon_3 < \tilde{\varepsilon}_0,\quad y \in S_2\},\\ \sigma_3^+ &= \{\rho_3 = \tilde{\rho}_3,\quad 0 \le \varepsilon_3 < \tilde{\varepsilon}_0,\quad y \in S_3\},\end{aligned}$$

where $\tilde{\varepsilon}_0 = \frac{\varepsilon_0}{\tilde{\rho}_3}$ and S_2 and S_3 are appropriate open intervals containing $\widetilde{y}$ and $\xi_X(\widetilde{y})$, respectively. The following Lemmas state properties of the transition maps $\Pi_{2,3,4}^+$. The smoothness of the flow of $\widetilde{Z}^{\varphi}_{\varepsilon,\widetilde{\alpha},\widetilde{\mu}}$ assures Lemma 7.

Lemma 7. *The transition map $\Pi_3^+ : \sigma_2^+ \to \sigma_3^+$, $(y,\varepsilon_3) \mapsto (\pi_3^+(y,\varepsilon_3,\widetilde{\alpha},\widetilde{\mu}),\varepsilon_3)$, is well defined and is C^∞.*

Proof. The transition map Π_3^+ is defined by following trajectories of (20) between the sections σ_2^+ and σ_3^+. Since we assumed that this passage is regular, Lemma 7 follows directly. □

The transition maps $\Pi_{2,4}^+$ were studied in [11] (see also [17, Subsection 4.2] and [18, Appendix B]). We state the properties that we need in the next Lemma.

Lemma 8. *Consider the transition maps $\Pi_2^+ : \sigma_1^+ \to \sigma_2^+$, $(y,\rho_3) \mapsto (\pi_2^+(y,\rho_3,\widetilde{\alpha},\widetilde{\mu}), \frac{\rho_3}{\tilde{\rho}_3\sqrt{\bar{x}_2}})$, and $\Pi_4^+ : \sigma_3^+ \to \sigma_4^+$, $(y,\varepsilon_3) \mapsto (\pi_4^+(y,\varepsilon_3,\widetilde{\alpha},\widetilde{\mu}), \tilde{\rho}_3\sqrt{\bar{x}_2}\varepsilon_3)$. Then given $r > 0$, there exist C^r-functions g_2^+ and g_4^+ such that*

$$\begin{aligned}\pi_2^+(y,\rho_3,\widetilde{\alpha},\widetilde{\mu}) = \pi_2^+\left(y,\varepsilon\sqrt{\bar{x}_2},\widetilde{\alpha},\widetilde{\mu}\right) &= g_2^+(y,\varepsilon,\varepsilon\ln\varepsilon^{-1},\widetilde{\alpha},\widetilde{\mu}),\\ \pi_4^+(y,\varepsilon_3,\widetilde{\alpha},\widetilde{\mu}) = \pi_4^+\left(y,\tfrac{\varepsilon}{\tilde{\rho}_3},\widetilde{\alpha},\widetilde{\mu}\right) &= g_4^+(y,\varepsilon,\varepsilon\ln\varepsilon^{-1},\widetilde{\alpha},\widetilde{\mu})\end{aligned}$$

where $0 \le \varepsilon < \varepsilon_0$, with $\varepsilon_0 > 0$ small enough.

Proof. Notice that $\Pi_{2,4}^+$ are related to the passage near the line $\rho_3 = \varepsilon_3 = 0$ (away from the tangency point) of saddle singularities with positive and negative eigenvalues of equal magnitude (see (20) and Subsection 3.5.2). This type of passage has been studied in [11]. □

Remark 9. In Lemma 8, we used the change of coordinates $\rho_3 = \varepsilon\sqrt{\bar{x}_2}$ on σ_1^+ and $\varepsilon_3 = \frac{\varepsilon}{\tilde{\rho}_3}$ on σ_3^+. This can be checked using the expressions of the transversal sections. We point out that $\pi_2^+(y,0,\widetilde{\alpha},\widetilde{\mu}) = g_2^+(y,0,0,\widetilde{\alpha},\widetilde{\mu})$ is the y-component of the intersection of the unstable manifold of the saddle singularity $(\rho_3,y,\varepsilon_3) = (0,y,0)$, $y \in S_1$, with the section σ_2^+. Similarly, the ω-limit point of the orbit of (20) through $(\rho_3,y,\varepsilon_3) = (\tilde{\rho}_3,y,0) \in \sigma_3^+$ is given by $(\rho_3,y,\varepsilon_3) = (0,\pi_4^+(y,0,\widetilde{\alpha},\widetilde{\mu}),0)$.

With completely analogous constructions, one can define the transversal sections σ_i^-, $i = 1,\dots,4$ on the left-hand side of the Figure 12(a). One also can state completely analogous statements for the transition maps $\Pi_i^- : \sigma_{i-1}^- \to \sigma_i^-$ as those given by the previous Lemmas (in backward time).

5.3. **Right and left-hand transition maps and difference map.** Now, we are able to define the *right* and *left-hand transition maps* $\Pi^\pm : \sigma_0 \to \sigma_5$ by

$$\Pi^\pm(y,\varepsilon) = \Pi_5^\pm \circ \Pi_4^\pm \circ \Pi_3^\pm \circ \Pi_2^\pm \circ \Pi_1^\pm(y,\varepsilon),$$

whose properties are given in the next proposition.

In what follows, we define the integrals

$$J_{\tilde{\mu}}^+(y) := I_5^+(\xi_X(y),\tilde{\mu}) < 0, \quad \text{and} \quad J_{\tilde{\mu}}^-(y) := I_5^-(\xi_Y(y),\tilde{\mu}) < 0, \tag{23}$$

where ξ_X and ξ_Y are the half return maps defined in Section 4 and $I_5^\pm$ are defined in (22).

Remark 10. Note that the derivative of $J_{\tilde{\mu}}^\pm$ with respect to the variable y is positive due to the chosen parametrization of σ_0.

Proposition 11. *The $\hat{y}$-components of the right- and left-hand transition maps $\Pi^\pm : \sigma_0 \to \sigma_5$, $(y,\varepsilon) \mapsto (\pi_{\tilde{\mu}}^\pm(y,\varepsilon,\widetilde{\alpha}),\varepsilon)$, are given by*

$$\pi_{\tilde{\mu}}^\pm(y,\varepsilon,\widetilde{\alpha}) = f_{\tilde{\mu}}^\pm(\varepsilon,\widetilde{\alpha}) - \exp\left(\frac{J_{\tilde{\mu}}^\pm(y) + o^\pm(1)}{\varepsilon^2}\right), \tag{24}$$

in which $f_{\tilde{\mu}}^\pm$ are smooth functions satisfying $(f_{\tilde{\mu}}^+ - f_{\tilde{\mu}}^-)(0,0) = 0$ and $\frac{\partial(f_{\tilde{\mu}}^+ - f_{\tilde{\mu}}^-)}{\partial\widetilde{\alpha}}(0,0) \neq 0$. In addition, $J_{\tilde{\mu}}^\pm$ are given by Equation (23). Finally, $o^\pm(1)$ tends to zero uniformly as $\varepsilon \to 0$.

Proof. Using Lemmas 4–8 and similar results in backward time, we see that the $\hat{y}$ component of the transition maps $\Pi^\pm$ can be written as (24). The properties of $f_{\tilde{\mu}}^+ - f_{\tilde{\mu}}^-$ follow from [6, Theorem 4] ($\widetilde{\alpha}$ is a regular breaking parameter and σ_5 is parameterized by the rescaled variable $\hat{y}$). The second component of $\Pi^\pm$ is clearly ε. □

Remark 12. In fact, the smooth function $f_{\tilde{\mu}}^+$ in Equation (24) is the smooth function f_5^+ given in Lemma 5. From now on, for the sake of simplicity, we work with the notation $f_{\tilde{\mu}}^+$. The same remark on the notation of $f_{\tilde{\mu}}^-$ and f_5^- holds.

Remark 13. Note that for $\varepsilon = 0$ the y-component of the composition $\Pi_4^\pm \circ \Pi_3^\pm \circ \Pi_2^\pm \circ \Pi_1^\pm$ in forward (resp. backward) time can be naturally identified with *the half return map ξ_X (resp. ξ_Y)*.

Define the *difference map* $\pi_{\tilde{\mu}}$ as $\pi_{\tilde{\mu}} = \pi_{\tilde{\mu}}^+ - \pi_{\tilde{\mu}}^-$. It follows from the construction that zeros of the difference map for $\varepsilon > 0$ correspond to periodic orbits of $\widetilde{Z}_{\varepsilon,\widetilde{\alpha},\widetilde{\mu}}^{\varphi}$. In what follows, we prove that zeros of $\pi_{\tilde{\mu}}$ are related to zeros of the slow divergence integral $J_{\tilde{\mu}}(y) = (J_{\tilde{\mu}}^+ - J_{\tilde{\mu}}^-)(y)$.

In summary, we prove that the slow divergence integral can indeed be applied in order to detect limit cycles of $\widetilde{Z}^{\varphi}_{\varepsilon,\widetilde{\alpha},\widetilde{\mu}}$.

In what follows, we say that a periodic orbit $\Upsilon^{y_i}_{\varepsilon,\widetilde{\mu}}$ is Hausdorff close to the limit periodic set Υ^{y_i} if $\Upsilon^{y_i}_{\varepsilon,\widetilde{\mu}} \to \Upsilon^{y_i}$ as $\varepsilon \to 0$ and $\widetilde{\mu} \to \widetilde{\mu}_0$ according to Hausdorff distance (see also [9, Section 4]).

Theorem C. (Terminal case) *Denote* $J_{\widetilde{\mu}}(y) = (J^+_{\widetilde{\mu}} - J^-_{\widetilde{\mu}})(y)$.

- **(a)** *Suppose that* $\widetilde{y} \in S_0$ *is a zero of multiplicity* k *of* $J_{\widetilde{\mu}_0}(y)$. *Then* $\widetilde{Z}^{\varphi}_{\varepsilon,\widetilde{\alpha},\widetilde{\mu}}$ *has at most* $k+1$ *limit cycles for* $\varepsilon > 0$ *sufficiently small,* $\widetilde{\alpha}$ *close to* 0 *and* $\widetilde{\mu}$ *kept near* $\widetilde{\mu}_0$, *which are Hausdorff close to* $\Upsilon^{\widetilde{y}}$.
- **(b)** *Assume that* $J_{\widetilde{\mu}_0}(y)$ *has exactly* k *simple zeros* $y_1 < \cdots < y_k$ *in* S_0. *Let* $y_0 \in S_0$ *satisfying* $y_0 < y_1$. *Then there is a smooth function* $\widetilde{\alpha} = \widetilde{\alpha}(\varepsilon, \widetilde{\mu})$ *satisfying* $\widetilde{\alpha}(0, \widetilde{\mu}) = 0$ *such that* $\widetilde{Z}^{\varphi}_{\varepsilon,\widetilde{\alpha}(\varepsilon,\widetilde{\mu}),\widetilde{\mu}}$ *has* $k+1$ *periodic orbits* $\Upsilon^{y_i}_{\varepsilon,\widetilde{\mu}}$, *with* $i = 0, \ldots, k$, *for each* $\varepsilon > 0$ *sufficiently small and* $\widetilde{\mu}$ *close to* $\widetilde{\mu}_0$. *In addition, for* $i = 0, \ldots, k$, *the periodic orbit* $\Upsilon^{y_i}_{\varepsilon,\widetilde{\mu}}$ *is isolated, hyperbolic and Hausdorff close to the canard cycle* Υ^{y_i}.

Proof. **Item (a).** By Rolle's Theorem, if $\pi'_{\widetilde{\mu}}(y, \varepsilon, \widetilde{\alpha})$ has k zeros counting multiplicity, then $\pi_{\widetilde{\mu}}(y, \varepsilon, \widetilde{\alpha})$ has at most $k+1$ zeros. In other words, if $\pi'_{\widetilde{\mu}}(y, \varepsilon, \widetilde{\alpha})$ has k zeros, then $\widetilde{Z}^{\varphi}_{\varepsilon,\widetilde{\alpha},\widetilde{\mu}}$ has at most $k+1$ limit cycles. The prime $'$ denotes the derivative with respect to y.

We write $\pi_{\widetilde{\mu}}(y) = \pi_{\widetilde{\mu}}(y, \varepsilon, \widetilde{\alpha})$. Using Proposition 11, one has that

$$\pi'_{\widetilde{\mu}}(y) = \exp\left(\frac{J^-_{\widetilde{\mu}}(y) + o^-(1)}{\varepsilon^2}\right)\frac{1}{\varepsilon^2}\frac{\partial}{\partial y}\Big(J^-_{\widetilde{\mu}} + o^-(1)\Big) - \exp\left(\frac{J^+_{\widetilde{\mu}}(y) + o^+(1)}{\varepsilon^2}\right)\frac{1}{\varepsilon^2}\frac{\partial}{\partial y}\Big(J^+_{\widetilde{\mu}} + o^+(1)\Big).$$

Now, using Remark 10, we can rewrite

$$\frac{1}{\varepsilon^2}\frac{\partial}{\partial y}\Big(J^{\pm}_{\widetilde{\mu}} + o^{\pm}(1)\Big) = \exp\left(\frac{\varepsilon^2 \ln(\frac{1}{\varepsilon^2}\frac{\partial}{\partial y}(J^{\pm}_{\widetilde{\mu}} + o^{\pm}(1)))}{\varepsilon^2}\right) = \exp\left(\frac{o^{\pm}(1)}{\varepsilon^2}\right),$$

and therefore

$$\pi'_{\widetilde{\mu}}(y) = \exp\left(\frac{J^-_{\widetilde{\mu}}(y) + o^-(1)}{\varepsilon^2}\right) - \exp\left(\frac{J^+_{\widetilde{\mu}}(y) + o^+(1)}{\varepsilon^2}\right),$$

where $o(1)^{\pm}$ tend to zero as ε tends to zero, uniformly in y, $\widetilde{\mu}$ and $\widetilde{\alpha}$.

It follows that, for $\varepsilon > 0$, $\pi'_{\widetilde{\mu}}(y) = 0$ if, and only if,

$$J^+_{\widetilde{\mu}}(y) - J^-_{\widetilde{\mu}}(y) + o(1) = 0, \tag{25}$$

in which $o(1) = o^+(1) - o^-(1)$. Since we assume that $\tilde{y}$ is a zero of multiplicity k of $J_{\widetilde{\mu}_0}$, then Equation (25) has at most k zeros (counting multiplicity) near $y = \tilde{y}$, for each $(\varepsilon, \widetilde{\alpha}, \widetilde{\mu})$ kept near $(0, 0, \widetilde{\mu}_0)$. This implies that $\pi'_{\widetilde{\mu}}(y)$ has at most k zeros (counting multiplicity) near $y = \tilde{y}$, for each $(\varepsilon, \widetilde{\alpha}, \widetilde{\mu})$ kept near $(0, 0, \widetilde{\mu}_0)$ and $\varepsilon > 0$. This completes the proof of Item (a).

Item (b). From Proposition 11 and the Implicit Function Theorem, it follows that there is a smooth function $\widetilde{\alpha}(\varepsilon, \widetilde{\mu})$ such that $\widetilde{\alpha}(0, \widetilde{\mu}) = 0$ and $(f^+_{\widetilde{\mu}} - f^-_{\widetilde{\mu}})\big(\varepsilon, \widetilde{\alpha}(\varepsilon, \widetilde{\mu})\big) = 0$ for $\varepsilon \geq 0$ sufficiently small. One can rewrite the difference map $\pi_{\widetilde{\mu}}$ as

$$\pi_{\widetilde{\mu}}\big(y, \varepsilon, \widetilde{\alpha}(\varepsilon, \widetilde{\mu})\big) = \exp\left(\frac{J^-_{\widetilde{\mu}}(y) + o^-(1)}{\varepsilon^2}\right) - \exp\left(\frac{J^+_{\widetilde{\mu}}(y) + o^+(1)}{\varepsilon^2}\right),$$

and $o^{\pm}(1) \to 0$ as $\varepsilon \to 0$, uniformly in y and $\widetilde{\mu}$. Therefore, zeros of $\pi_{\widetilde{\mu}}\big(y, \varepsilon, \widetilde{\alpha}(\varepsilon, \widetilde{\mu})\big)$ with respect to the y variable are given by

$$J^{-}_{\widetilde{\mu}}(y) - J^{+}_{\widetilde{\mu}}(y) + o(1) = 0,$$

with $o(1) = o^{-}(1) - o^{+}(1)$ and obviously $o(1) \to 0$ as $\varepsilon \to 0$, uniformly in y and $\widetilde{\mu}$. Suppose that $y_1, \ldots, y_k \in S_0$ are simple zeros of $J_{\widetilde{\mu}_0}(y)$, and write $y_1 < \cdots < y_k$. For $\varepsilon > 0$ sufficiently small, those simple zeros persist, and therefore we have k simple zeros of the difference map $\pi_{\widetilde{\mu}}\big(y, \varepsilon, \widetilde{\alpha}(\varepsilon, \widetilde{\mu})\big)$. Finally, we conclude that $\widetilde{Z}^{\varphi}_{\varepsilon, \widetilde{\alpha}(\varepsilon,\widetilde{\mu}), \widetilde{\mu}}$ has k hyperbolic limit cycles $\Upsilon^{y_i}_{\varepsilon,\widetilde{\mu}}$, each one Hausdorff close to the canard cycle Υ^{y_i}, for $i = 1, \ldots, k$.

Fix $y_0 \in S_0$ such that $y_0 < y_1$. Using suitable functions $f^{\pm}_{\widetilde{\mu}}$ (see [10, 12] for more details), it is possible to construct one extra hyperbolic limit cycle $\Upsilon^{y_0}_{\varepsilon,\widetilde{\mu}}$, and it will be the smallest limit cycle among $\Upsilon^{y_i}_{\varepsilon,\widetilde{\mu}}$, for $i = 0, \ldots, k$. □

Remark 14. In [10, 12], a result similar to Theorem C(b) has been proven for red canard cycles in Figure 1(b). More precisely, in our model (15) such canard cycles can be parameterized by $y \in (0, y^*)$ where we suppose that the slow dynamics (18) along the portion of the critical curve C_0 below the line $y = y^*$ is regular (that is, negative). We define the following slow divergence integrals: $\overline{I}^{+}_{\widetilde{\mu}}(y) < 0$ (resp. $\overline{I}^{-}_{\widetilde{\mu}}(y) < 0$), equal to the integral $I^{+}_{\widetilde{\mu}}(x_2)$ (resp. $I^{-}_{\widetilde{\mu}}(x_2)$) defined in (19), where x_2 is the x_2-coordinate of the ω-limit point (resp. α-limit point) of the fast orbit of (17) through $(x_2, y) = (0, y)$. Now, if $\overline{I}^{+}_{\widetilde{\mu}_0}(y) - \overline{I}^{-}_{\widetilde{\mu}_0}(y)$ has exactly k simple zeros in the open interval $(0, y^*)$, we can produce $k + 1$ limit cycles like in our Theorem C(b). An important difference lies in the fact that the extra limit cycle found in [10, 12] is the biggest, that is, the extra limit cycle surrounds the k limit cycles obtained from the simple zeros. On the other hand, in our Theorem C(b), the extra limit cycle is the smallest one.

5.4. **Proof of Theorem A.** We consider a PSVF presenting a non-smooth center at $(0, 1) \in \Sigma$ given by

$$Z_{\alpha}(x, y) = \begin{cases} X_{\alpha}(x, y) &= \big(y - 1, \alpha - 1\big), \\ Y_{\alpha}(x, y) &= \big(y - 1, \alpha + 1\big). \end{cases} \tag{26}$$

Let $\widetilde{Z}_{\alpha}$ be a continuous combination of (26) given by

$$\widetilde{Z}_{\alpha}(\lambda, x, y) = \begin{cases} \widetilde{Z}_1(\lambda, y) &= y - \lambda^2, \\ \widetilde{Z}_{2,\alpha}(\lambda) &= \alpha - \lambda. \end{cases} \tag{27}$$

Observe that the continuous combination (27) is a special case of (8) with $\mu = \alpha$ (we do not need the additional parameter $\widetilde{\mu}$) and $A_{\mu} = B_{\mu} \equiv 0$. The associated functions F and G (defined in (12)) are given by $F(x) = \varphi^2(x)$ and $G(x) = -\varphi(x)$. The critical curve C_0 is equal to $\{y = F(x_2)\}$ (see Section 3.5.1). We assume that $\varphi(0) = 0$ and $\varphi'(0) > 0$ (see the assumption **(A0)**). Moreover, in this section we assume that transition functions are monotonic. Then the assumptions **(A2)** and **(A3)** are satisfied on the interval $(-1, 1)$. Since $A_{\mu} \equiv 0$, then assumption **(A1)** is satisfied.

We focus on limit cycles of the following non-linear regularization (see (15)):

$$\widetilde{Z}^{\varphi}_{\varepsilon,\widetilde{\alpha}}(x, y) := \widetilde{Z}_{\varepsilon\widetilde{\alpha}}\Big(\varphi\Big(\frac{x}{\varepsilon^2}\Big), x, y\Big) = \begin{cases} \dot{x} &= y - \varphi^2\left(\frac{x}{\varepsilon^2}\right), \\ \dot{y} &= \varepsilon\widetilde{\alpha} - \varphi\left(\frac{x}{\varepsilon^2}\right). \end{cases}$$

In addition, the half return maps of Z_0 in (26) are given by $\xi_{X,Y}(y) = 2 - y$ and $\xi(y) = y$, see assumption **(A4)** in the terminal case (recall that ξ_Y is considered in backward time,

see also Figure 9). Note that the canard cycle Υ^y (see Figure 10(a)) is well-defined for each $y \in (1,2)$. We therefore restrict the half return maps to the interval $(1,2)$.

Our goal is to show that for any integer $k > 0$ there exists a monotonic function φ_k such that the slow divergence integral J from Theorem C(b) has k simple zeros $1 < y_1 < \cdots < y_k < 2$.

Let us first find the expression for J. From (22) and (23) it follows that

$$J(y) = I^+(x_2^+(2-y)) - I^-(x_2^-(2-y)),$$

where $I^\pm$ are defined in (19) (recall that we do not have parameter $\widetilde{\mu}$). If we use the change of variable $x = x_2^+(2-y)$ and write $J(y)$ as $I(x)$, then we have

$$I(x) = I^+(x) - I^-(L(x)) = 4\int_x^{L(x)} \varphi(s)\big(\varphi'(s)\big)^2 ds, \tag{28}$$

where $x \in (0,1)$ and $L(x) < 0$ satisfies $\varphi^2(x) = \varphi^2(L(x))$, due to $\xi(y) = y$. Now, it suffices to prove that for any integer $k > 0$ there is a monotonic function φ_k such that I has k (positive) simple zeros.

Consider a function $\widetilde{\varphi}(x) = x + \delta\varphi_e(x)$, in which φ_e is an even polynomial satisfying $\varphi_e(0) = 0$. We fix a compact interval $[-2\nu, 2\nu] \subset (-1,1)$, with a small $\nu > 0$. The function $\widetilde{\varphi}$ is monotonic in $[-2\nu, 2\nu]$ for any $\delta \geq 0$ sufficiently small. Using the definition of $\widetilde{\varphi}$ and $\widetilde{\varphi}^2(x) = \widetilde{\varphi}^2(L(x))$, one can also write $L(x) = -x + L_1(x)\delta + O(\delta^2)$, where $L_1(x) = -2\varphi_e(x)$.

Therefore, for $x \in (0, \nu]$ and $\delta \geq 0$ sufficiently small, we have

$$\begin{aligned}
\frac{1}{4}I(x) &= \int_x^{L(x)} \widetilde{\varphi}(s)\big(\widetilde{\varphi}'(s)\big)^2 ds = \int_x^{L(x)} \big(s + \delta\varphi_e(s)\big)\big(1 + \delta\varphi_e'(s)\big)^2 ds \\
&= \int_x^{L(x)} s ds + \delta\int_x^{L(x)} \big(2s\varphi_e'(s) + \varphi_e(s)\big) ds + O(\delta^2) \\
&= -\delta x L_1(x) + \delta\int_x^{-x} \big(2s\varphi_e'(s) + \varphi_e(s)\big) ds + O(\delta^2).
\end{aligned}$$

Observe that $2s\varphi_e'(s) + \varphi_e(s)$ is an even polynomial. Thus

$$\int_x^{-x} \big(2s\varphi_e'(s) + \varphi_e(s)\big) ds = -2\int_0^x \big(2s\varphi_e'(s) + \varphi_e(s)\big) ds,$$

because we are integrating in a symmetric interval. We also remark that

$$\int_0^x s\varphi_e'(s) ds = x\varphi_e(x) - \int_0^x \varphi_e(s) ds,$$

and then we finally have

$$\frac{1}{4}I(x) = -2\delta\int_0^x s\varphi_e'(s) ds + O(\delta^2). \tag{29}$$

We conclude that simple zeros of the integral in the right hand side of (29) will persist as simple zeros of $I(x)$, for each small but positive δ.

Given any positive integer k, take $a_1 < \cdots < a_k$ in the open interval $(0, \nu)$. Define the odd polynomial $P(x) = x^3(x^2 - a_1^2)\ldots(x^2 - a_k^2)$. The even polynomial $\varphi_e(x) = \int_0^x \frac{P'(s)}{s} ds$ satisfies $\int_0^x s\varphi_e'(s) ds = P(x)$ and therefore the integral in the right hand side of (29) has k simple zeros $a_1 < \cdots < a_k$ in $(0, \nu)$. They persist as simple zeros of $I(x)$ in $(0, \nu)$, for positive but small δ.

The next step is to smoothly extend $\widetilde{\varphi}(x)$ to a monotonic transition function φ_k in the interval $[-1, 1]$. Define a *bump function* $\beta : \mathbb{R} \to \mathbb{R}$ with support $\mathrm{supp}(\beta) = (-2, 2)$ and

satisfying $\beta(x) \equiv 1$ in the compact interval $[-1,1]$. Now, define $\beta_\nu(x) = \beta\left(\frac{x}{\nu}\right)$. With this construction, we have $\text{supp}(\beta_\nu) = (-2\nu, 2\nu)$ and $\beta_\nu \equiv 1$ in the compact interval $[-\nu,\nu]$. Finally, using the monotonic transition function

$$\psi(x) = \begin{cases} \tanh\left(\frac{x}{1-x^2}\right) & \text{if} \quad |x| < 1, \\ \operatorname{sgn} x & \text{if} \quad |x| \geq 1, \end{cases}$$

we define $\varphi_k(x) = \widetilde{\varphi}(x)\beta_\nu(x) + \psi(x)\left(1 - \beta_\nu(x)\right)$.

We claim that φ_k is a monotonic transition function. Indeed, observe that ψ, β_ν and consequently φ_k are C^∞-smooth functions. Furthermore, $\varphi_k \equiv \widetilde{\varphi}$ and $\varphi_k \equiv \psi$ in $[-\nu,\nu]$ and $(-\infty,-2\nu] \cup [2\nu,\infty)$, respectively. Therefore, it remains to check that φ_k is monotonic in $(-2\nu,-\nu) \cup (\nu,2\nu)$. In order to do this, we can proceed as in the proof of [18, Theorem 4.3] because $\widetilde{\varphi}(0) = \psi(0) = 0$ and $\widetilde{\varphi}'(0) = \psi'(0) = 1$.

Now Theorem A follows directly from Theorem C(b). The $k+1$ limit cycles are produced by the canard cycles Υ^y (see Figure 10(a)). Bearing in mind Remark 14, these $k+1$ limit cycles can also be produced by red canard cycles in Figure 1(b). Indeed, we have the same integral $I(x)$ as above and we can construct k simple zeros using the same steps (see also Section 5.5). The $k+1$ red limit cycles (as in Figure 1(b)) occur for a new control curve $\widetilde{\alpha} = \widetilde{\alpha}(\varepsilon)$. □

5.5. **Proof of Theorem B.** Consider the linear PSVF (for $\alpha \sim 0$)

$$Z_\alpha(x,y) = \begin{cases} X_\alpha(x,y) = \big(y - 1 - \alpha, \quad \alpha - 1 - x\big), \\ Y_\alpha(x,y) = \big(y - 1 - x, \quad \alpha + 1 - x\big). \end{cases} \tag{30}$$

Let us describe the phase portrait of Z_α. The points $P_\alpha = (-1+\alpha, 1+\alpha)$ and $Q_\alpha = (1+\alpha, 2+\alpha)$ are (virtual) linear center and attracting focus of X_α and Y_α, respectively. It can also be checked that both $T_\alpha^X = (0, 1+\alpha)$ and $T_\alpha^Y = (0,1)$ are invisible fold points. Geometrically, it is easy to see that, for $\alpha = 0$, the fold-fold singularity behaves like a non-smooth attracting focus, because Y_α has a smooth attracting focus. The segment limited by these fold points is the sliding region Σ^s, and the sewing region is given by $\Sigma^w = \Sigma \backslash \left(\Sigma^s \cup T_\alpha^X \cup T_\alpha^Y\right)$.

In order to verify that the invisible-invisible fold-fold $(0,1) \in \Sigma$ has codimension 1, we must compute $\xi_{X,Y}$. One can explicitly solve the system of ODEs associated to X_0 and obtain $\xi_X(y) = 2 - y$. Using Taylor series of order 2 of the solutions of Y_0, we obtain

$$\xi_Y^{-1}(y) = \frac{-y^3 + 4y^2 - 8y + 6}{(y-2)^2}.$$

Therefore

$$\begin{aligned} \xi(y) &= \xi_Y^{-1} \circ \xi_X(y) = -\tfrac{2}{y^2} + \tfrac{4}{y} + y - 2 \\ &= 1 + (y-1) - 2(y-1)^2 + 4(y-1)^3 - 6(y-1)^4 + O\left((y-1)^5\right). \end{aligned}$$

The coefficient of $(y-1)^2$ is nonzero, therefore this singularity has codimension 1. Moreover, such coefficient is negative, therefore this II_2 has an attracting focus-like behavior.

A continuous combinations of (30) is given by

$$\widetilde{Z}_\alpha(\lambda,x,y) = \left(y - \lambda^2 - \frac{(\alpha - x)\lambda^{m-1}}{2} - \frac{(\alpha + x)\lambda^m}{2}, \quad \alpha - \lambda - x\lambda^n\right), \tag{31}$$

with $m \geq 4$ and $n \geq 2$ being even integers. The continuous combination (31) is a special case of (8) with $\mu = \alpha$, $A_\alpha(\lambda,x) = -\frac{(\alpha-x)\lambda^{m-1}}{2} - \frac{(\alpha+x)\lambda^m}{2}$ and $B_\alpha(\lambda,x,y) = -x\lambda^n$. Using (12), one obtains $F(x) = \varphi^2(x)$ and $G(x) = -\varphi(x)$. The critical curve C_0 is given by $\{y = F(x)\}$. Assuming that φ is monotonic and $\varphi(0) = 0$, then the assumptions **(A0)-(A3)** are satisfied.

In what follows, we focus on red canard cycles in Figure 1(b) of the regularization (15). We believe that the same result is true for big limit cycles (see Figure 10(a)). This case is more technical and it is a topic of further study.

Using Remark 14 and parameterizing the slow divergence integrals by $x \in (0,1)$ instead of $y \in (0,1)$ (we use the change of variable $y = F(x)$), it suffices to study simple zeros of

$$I(x) = 4 \int_x^{L(x)} \varphi(s) \left(\varphi'(s)\right)^2 ds,$$

where $x \in (0,1)$, $L(x) < 0$ and $F(x) = F(L(x))$. This slow divergence integral has the same form as (28) in the non-smooth center case. Using the same reasoning as in Section 5.4 we can show that for any integer $k > 0$ there is a monotonic function φ_k such that I has k (positive) simple zeros. Finally, Remark 14 implies that $k+1$ hyperbolic limit cycles can be produced inside the regularization stripe. □

6. Analysis of the dodging case

In this section we consider the dodging case defined in Section 4 (we suppose that the assumptions **(A0-4)** are satisfied). In this case, the slow divergence integral can also be used in order to study limit cycles of the regularized vector field defined in (15), produced by canard cycles $\Gamma^{\widetilde{y}}$ in Figure 10(b).

Of course, one must define transversal sections and transition maps for this case. We will not go into details since the construction, lemmas and propositions can be done in an analogous way as it was done in Section 5. We refer to Figure 12(b) for the transversal sections σ_i^- for $i = 0, \ldots, 5$. We use the same parameterization of $\sigma_{0,5}$ as in Section 5.1.

The $\hat{y}$-components of the transition maps $\Pi^{\pm} : \sigma_0 \to \sigma_5$ are given by

$$\begin{aligned} \pi^+_{\widetilde{\mu}}(y,\varepsilon,\widetilde{\alpha}) &= f^+_{\widetilde{\mu}}(\varepsilon,\widetilde{\alpha}) + \exp\left(\frac{\overline{I}^+_{\widetilde{\mu}}(y) + o^+(1)}{\varepsilon^2}\right), \\ \pi^-_{\widetilde{\mu}}(y,\varepsilon,\widetilde{\alpha}) &= f^-_{\widetilde{\mu}}(\varepsilon,\widetilde{\alpha}) - \exp\left(\frac{J^-_{\widetilde{\mu}}(y) + o^-(1)}{\varepsilon^2}\right), \end{aligned} \tag{32}$$

in which the smooth functions $f^{\pm}_{\widetilde{\mu}}$ and $o^{\pm}(1)$ satisfy analogous properties to Proposition 11, $J^-_{\widetilde{\mu}}(y)$ is defined in (23) and $\overline{I}^+_{\widetilde{\mu}}(y)$ in Remark 14. The expression for $\pi^-_{\widetilde{\mu}}$ follows from (24), while the expression for $\pi^+_{\widetilde{\mu}}$, together with the properties of $f^+_{\widetilde{\mu}} - f^-_{\widetilde{\mu}}$ stated in Proposition 11, follows from [6, Theorem 4]. Observe that we have a plus sign in front of the exponential in the expression of $\pi^+_{\widetilde{\mu}}$. The difference map is then given by $\pi_{\widetilde{\mu}} = \pi^+_{\widetilde{\mu}} - \pi^-_{\widetilde{\mu}}$ and the derivative of $\overline{I}^+_{\widetilde{\mu}}(y)$ with respect to y is negative, due to the chosen parameterization of σ_0. See also Remark 10.

We have the following result.

Theorem D. (Dodging case) *Denote $I_{\widetilde{\mu}}(y) = (\overline{I}^+_{\widetilde{\mu}} - J^-_{\widetilde{\mu}})(y)$, and let $\widetilde{y} \in S_0$. Then $\widetilde{Z}^{\varphi}_{\varepsilon,\widetilde{\alpha},\widetilde{\mu}}$ has at most 2 limit cycles produced by the canard cycle $\Gamma^{\widetilde{y}}$, for $\varepsilon > 0$ sufficiently small, $\widetilde{\alpha}$ close to zero and $\widetilde{\mu}$ close to $\widetilde{\mu}_0$. Moreover, if $y = \widetilde{y}$ is a simple root of $I_{\widetilde{\mu}_0}(y)$, then, for each $\varepsilon > 0$ sufficiently small and $\widetilde{\mu}$ close to $\widetilde{\mu}_0$, the $\widetilde{\alpha}$-family $\widetilde{Z}^{\varphi}_{\varepsilon,\widetilde{\alpha},\widetilde{\mu}}$ undergoes a saddle-node bifurcation of limit cycles, which are Hausdorff close to $\Gamma^{\widetilde{y}}$.*

Proof. Firstly, we prove the existence of at most two limit cycles. With reasoning and notation similar to those in the proof of Theorem C(a), one can show that, for each small

$\varepsilon > 0$, $\pi'_{\widetilde{\mu}}(y) = 0$ is equivalent to

$$\overline{I}^{+}_{\widetilde{\mu}}(y) - J^{-}_{\widetilde{\mu}}(y) + o(1) = 0, \tag{33}$$

where $o(1) \to 0$ as $\varepsilon \to 0$. Notice that the derivative of the left hand side of (33) with respect to y is negative for each $\varepsilon \geq 0$ small enough (we use Remark 10 and the fact that the derivative of $\overline{I}^{+}_{\widetilde{\mu}}$ is negative). Rolle's Theorem implies that (33) has at most 1 solution (counting multiplicity) near $y = \widetilde{y}$. Thus, $\pi'_{\widetilde{\mu}}(y)$ has at most 1 zero near $y = \widetilde{y}$. Applying Rolle's Theorem once more, we conclude that $\Gamma^{\widetilde{y}}$ can produce at most 2 limit cycles. This completes the proof of the first part of Theorem D. The second part of Theorem D can be proved in the same fashion as Theorem 4.3(3) in [12].

□

7. Acknowledgements

The authors thank the anonymous referee for the valuable comments that helped to improve the presentation of this paper.

Peter De Maesschalck is supported by Flanders FWO agency (G0F1822N grant). Renato Huzak is supported by Croatian Science Foundation (HRZZ) grant IP-2022-10-9820. Otavio Henrique Perez is supported by Sao Paulo Research Foundation (FAPESP) grants 2021/10198-9 and 2024/00392-0.

8. Conflict of interest

On behalf of all authors, the corresponding author states that there is no conflict of interest.

References

[1] di Bernardo, M., Budd, C.J., Champneys, A.R., Kowalczyk, P. *Piecewise-Smooth Dynamical Systems: Theory and Applications*. **Springer Verlag London Ltd.**, London (2008).

[2] C. Bonet-Reves, J. Larrosa, T.M. Seara. *Regularization around a generic codimension one fold-fold singularity*. **J. Diff. Eq.** 265 (2018), 1761–1838.

[3] E. Bossolini, M. Brøns, and K. U. Kristiansen. *Canards in stiction: on solutions of a friction oscillator by regularization*. **SIAM Journal on Applied Dynamical Systems** 16(4) (2017).

[4] C. Buzzi, P.R. Silva, M.A. Teixeira. *A singular approach to discontinuous vector fields on the plane*. **J. Diff. Eq.** 231 (2006), 633–655.

[5] C. Buzzi, T. Carvalho, M.A. Teixeira. *Birth of limit cycles bifurcating from a nonsmooth center*. **J. Math. Pures Appl.** 102 (2014), 36–47.

[6] P. De Maesschalck, F. Dumortier. *Time analysis and entry-exit relation near planar turning points*. **J. Diff. Eq.** 215(2) (2005), 225–267.

[7] P. De Maesschalck, F. Dumortier. *Canard solutions at non-generic turning points*. **Trans. Amer. Math. Soc.** 358(5) (2005), 2291–2334.

[8] P. De Maesschalck, F. Dumortier. *Canard cycles in the presence of slow dynamics with singularities*. **Proc. Roy. Soc. Edinburgh Sect. A** 138 (2008), 265–299.

[9] P. De Maesschalck, F. Dumortier, R. Roussarie. *Canard cycles—from birth to transition*, volume 73 of Ergebnisse der Mathematik und ihrer Grenzgebiete. 3. Folge. A Series of Modern Surveys in Mathematics [Results in Mathematics and Related Areas. 3rd Series. A Series of Modern Surveys in Mathematics]. Springer, Cham, (2021).

[10] P. De Maesschalck, R. Huzak. *Slow divergence integrals in classical Liénard equations near centers*. **J. Dyn. Diff. Eq.** 27(1) (2015), 177–185.

[11] P. De Maesschalck, S. Schecter. *The entry-exit function and geometric singular perturbation theory*. **J. Diff. Eq.** 260(8) (2016), 6697–6715.

[12] F. Dumortier. *Slow divergence integral and balanced canard solutions*. **Qual. Theory Dyn. Syst.** 10(1) (2011), 65–85.
[13] F. Dumortier, D. Panazzolo, R. Roussarie. *More limit cycles than expected in Liénard equations*. **Proc. Am. Math. Soc.** 135(6) (2007), 1895–1904.
[14] F. Dumortier, R. Roussarie. *Canard cycles and center manifolds*. **Mem. Am. Math. Soc.** 121(577), x+100 (1996). (With an appendix by Cheng Zhi Li)
[15] A.F. Filippov. *Differential Equations with Discontinuous Right-Hand Sides*. Mathematics and Its Applications (Soviet Series), Kluwer Academic Publishers, Dordrecht, 1988.
[16] M. Guardia, T.M. Seara, M.A. Teixeira. *Generic bifurcations of low codimension of planar Filippov Systems*. **J. Diff. Eq.** 250 (2011), 1967–2023.
[17] I. Gucwa, P. Szmolyan. *Geometric singular perturbation analysis of an autocatalator model*. **Discrete Contin. Dyn. Syst., Ser**. S 2(4) (2009), 783–806.
[18] R. Huzak, K.U. Kristiansen. *The number of limit cycles for regularized piecewise polynomial systems is unbounded*. **J. Diff. Eq.** 342 (2023), 34–62.
[19] R. Huzak, K.U. Kristiansen. *Sliding Cycles of Regularized Piecewise Linear Visible–Invisible Twofolds*. **Qual. Theory Dyn. Syst.** 23 (Suppl 1), 256 (2024).
[20] R. Huzak, K.U. Kristiansen, G. Radunovic. *Slow divergence integral in regularized piecewise smooth systems*. **Electron. J. Qual. Theory Differ. Equ.** Paper No. 15, 20 p. (2024).
[21] M. Jeffrey. *Hidden Dynamics: The Mathematics of switches, decisions and other discontinuous behaviour*. Springer Nature Switzerland AG (2018).
[22] D. Joyce. *A generalization of manifold with corners*. **Adv. Math.** 299 (2016), 760–862.
[23] K.U. Kristiansen, S.J. Hogan. *Regularizations of two-fold bifurcations in planar piecewise smooth systems using blowup*. **SIAM J. Applied Dyn. Syst.** 14(4) (2015), 1731–1786.
[24] Yu.A. Kuznetsov, S. Rinaldi, A. Gragnani. *One-parameter bifurcations in planar Filippov systems*. **Internat. J. Bifur. Chaos Appl. Sci. Engrg.** 13(8) (2003), 2157–2188.
[25] D.D. Novaes, M.R. Jeffrey. *Regularization of hidden dynamics in piecewise smooth flows*. **J. Diff. Eq.** 259 (2015), 4615–4633.
[26] D. Panazzolo, P.R. da Silva. *Regularization of discontinuous foliations: Blowing up and sliding conditions via Fenichel Theory*. **J. Diff. Eq.** 263 (2017), 8362–8390.
[27] O.H. Perez, G. Rondón, P.R. da Silva. *Slow-Fast Normal Forms Arising from Piecewise Smooth Vector Fields*. **J. Dyn. Control Syst.** 29 (2023), 1709–1726.
[28] P.R. da Silva, I.S. Meza-Sarmiento, D.D. Novaes. *Nonlinear Sliding of Discontinuous Vector Fields and Singular Perturbation*. **Diff. Eq. Dyn. Syst.** 30 (2022), 675–693.
[29] J. Sotomayor, A.L.F. Machado. *Structurally stable discontinuous vector fields in the plane*. **Qual. Theory Dyn. Syst.** 3 (1) (2002), 227–250.
[30] J. Sotomayor, M.A. Teixeira. *Regularization of discontinuous vector fields*. International Conference on Differential Equations, Lisboa, 1996, 207–223.
[31] J. Yao, J. Huang, R. Huzak. *Cyclicity of slow-fast cycles with two canard mechanisms*. **Chaos** 34, 053112 (2024).
[32] J. Yao, J. Huang, R. Huzak, S. Ruan. *Cyclicity of slow–fast cycles with one self-intersection point and two nilpotent contact points*. **Nonlinearity** 37, 115007 (2024).

[1]Hasselt University, Campus Diepenbeek, Agoralaan Gebouw D, 3590 Diepenbeek, Belgium

[2]Universidade de São Paulo (USP), Instituto de Ciências Matemáticas e de Computação (ICMC). Avenida Trabalhador São Carlense, 400, CEP 13566-590, São Carlos, São Paulo, Brazil.

Email address: peter.demaesschalck@uhasselt.be
Email address: renato.huzak@uhasselt.be
Email address: otavio.perez@icmc.usp.br